Plant Cell Tiss Organ Cult (2017) 131:579–599
DOI 10.1007/s11240-017-1308-2

ORIGINAL ARTICLE

Molecular cloning and functional analysis of *DoUGE* related to water-soluble polysaccharides from *Dendrobium officinale* with enhanced abiotic stress tolerance

Zhenming Yu[1,2] · Chunmei He[1] · Jaime A. Teixeira da Silva[3] · Guihua Zhang[1,2] · Wei Dong[1] · Jianping Luo[4] · Jun Duan[1,2]

Received: 14 March 2017 / Accepted: 12 September 2017 / Published online: 20 September 2017

Abstract UDP glucose 4-epimerase (UGE), an enzyme with significant impacts on sugar metabolism, catalyzes the reversible inter-conversion between UDP-glucose and UDP-galactose. However, very little is known about whether UGE plays a critical role in the accumulation of water-soluble polysaccharide (WSP) and its relationship to abiotic stress tolerance. Here, *DoUGE* from *D. officinale*, encoding UGE localized in the cytoplasm, was initially cloned and analyzed. *DoUGE* exhibited highly tissue-specific expression patterns. The highest expression was in the stems of seedlings and adult plants. The content of WSPs ranged from 168.43 to 416.12 mg g^{-1} DW from developmental stages S1 to S4, the highest value being in S3. *DoUGE* was expressed throughout S1 to S4, with a maximum in S3. This trend was similar in three cultivated varieties (T10, T32-5 and T636). There was a positive correlation between *DoUGE* expression and the content of WSPs ($R^2 = 0.94$; $p < 0.01$). Furthermore, promoter analysis showed its possible role in responses to abiotic stresses. Transgenic *Arabidopsis thaliana* seedlings overexpressing *DoUGE* accumulated 34.84–44.78% more WSPs, showed 26.24–32.79% more UGE activity, and had a 1.19–1.31-fold higher chlorophyll content than the wild type. Transgenic plants also showed a 50.84 and 34.33% increase in the average content of glucose and galactose, respectively. Transgenic lines growing in half-strength Murashige and Skoog medium containing 150 mM NaCl or 200 mM mannitol displayed enhanced root length and fresh weight, as well as lower proline and malondialdehyde accumulation under salt and osmotic stresses, indicating that the *DoUGE* gene could be used to improve tolerance to abiotic stress in crops and medicinal or ornamental plants. Our results provide genetic evidence for the involvement of *DoUGE* in the regulation of WSP content during plant development in *D. officinale*, as well as in enhanced tolerance to salt and osmotic stresses.

Keywords UDP glucose 4-epimerase · *Dendrobium officinale* · Quantitative real-time PCR · Abiotic stress · Water-soluble polysaccharides

Abbreviations

CaMV	*Cauliflower mosaic virus*
DoCSLA	The gene encoding cellulose synthase-like A from *D. officinale*
DoUGE	The gene encoding UGE from *D. officinale*
DW	Dry weight
GSP	Gene-specific primers
HPLC	High performance liquid chromatography
MAT	Months after transplantation
MDA	Malondialdehyde
MS	Murashige and Skoog medium (1962)

Communicated by T. Winkelmann.

Electronic supplementary material The online version of this article (doi:10.1007/s11240-017-1308-2) contains supplementary material, which is available to authorized users.

✉ Jun Duan
duanj@scib.ac.cn

[1] Key Laboratory of South China Agricultural Plant Molecular Analysis and Gene Improvement, South China Botanical Garden, Chinese Academy of Sciences, Guangzhou 510650, China

[2] University of Chinese Academy of Sciences, Beijing 100049, China

[3] P. O. Box 7, Miki-cho Post Office, Ikenobe 3011-2, Miki-cho, Kita-gun, Kagawa-ken 761-0799, Japan

[4] School of Food Science and Engineering, Hefei University of Technology, Hefei 230009, China

NJ	Neighbor-joining method (Saitou and Nei 1987)
ORF	Open reading frame
PMP	1-Phenyl-3-methyl-5-pyrazolone
PPFD	Photosynthetic photon flux density
qRT-PCR	Quantitative real-time PCR
RACE	Rapid-amplification of cDNA ends
SA	Salicylic acid
SDR	Short-chain dehydrogenase/reductase
UGE	UDP glucose 4-epimerase
WSP	Water-soluble polysaccharide
WT	Wild type
YFP	Yellow fluorescence protein

Introduction

UDP glucose 4-epimerase (UGE, EC 5.1.3.2), which belongs to the short-chain dehydrogenase/reductase (SDR) superfamily and is one of the enzymes in the Leloir pathway (Reiter and Vanzin 2001), catalyzes the freely reversible interconversion of UDP-glucose to UDP-galactose (Maitra and Ankel 1971). The SDR superfamily enzymes participate in numerous physiological and biochemical processes, including fertility, hypertension, and neoplastic processes (Holden et al. 2003), all of which also play a part in the biosynthesis of different polysaccharide structures (Beerens et al. 2015). UDP-glucose and UDP-galactose, which are synthesized in the cytosol by UGE then transferred to the Golgi apparatus, are involved in the synthesis of cell wall polysaccharides (Yin et al. 2011). The gene encoding the UGE protein has been widely isolated from microorganism and animals, but less so from plants (Dormann and Benning 1998).

There are multiple natural biological functions of UGE in plants, animals, and microorganisms. Our group focuses primarily on the roles of UGE in response to abiotic stresses and in carbohydrate metabolism. A family of five genes encoding UGE isolated from *A. thaliana* is involved in the regulation of cell wall polysaccharide biosynthesis (Barber et al. 2006; Rosti et al. 2007). *AtUGE1* and *AtUGE3* mainly participate in carbohydrate metabolism, while *AtUGE2, AtUGE4* and *AtUGE5* are associated with the accumulation of carbohydrates (Barber et al. 2006). Overexpression of *AtUGE2* enhances the content of cell wall galactan and galactose, and helps to increase biomass without altering plant growth and development (Gondolf et al. 2014). *AtUGE1* and *AtUGE5* provide plants with resistance against abiotic stresses such as high salt, low temperature and drought (Rosti et al. 2007). In addition, four *UGE*s (*OsUGE1-4*) from *Oryza sativa* have been sequenced: these OsUGEs produce different forms of UDP-sugars such as UDP-glucose, UDP-galactose, UDP-xylose and UDP-arabinose (Kim et al. 2009). *OsUGE1* overexpression can improve tolerance to salt, drought and freezing, which may be associated with the enhanced accumulation of raffinose (Liu et al. 2007). *OsUGE1* is helpful for the transport of carbohydrate polysaccharides (Guevara et al. 2014). However, there is no evidence that the *UGE* gene is associated with the biosynthesis of water-soluble polysaccharides (WSPs). Furthermore, the gene encoding UGE in *D. officinale* has not been investigated, and the role of *DoUGE* in abiotic stress tolerance and WSP synthesis is unclear in orchid plants.

Dendrobium officinale, which is a perennial epiphytic orchid, has a wealth of WSPs that are primarily mannan polysaccharides, including glucomannan and galactoglucomannan (Ng et al. 2012; Xing et al. 2013). A biosynthetic pathway for glucomannan and galactoglucomannan exists in *Trigonella foenum-graecum* (Wang et al. 2012) and *D. officinale* (Zhang et al. 2016a), indicating that UGE is involved in mannan biosynthesis. Moreover, UGE plays a role in providing UDP-galactose for galactosylation (Seifert et al. 2002), and UDP-galactose is used for galactomannan biosynthesis (Wang et al. 2012). Several genes that are involved in the mannan biosynthetic pathway in *D. officinale* showing homology with genes in the *A. thaliana* genome have been isolated, including the alkaline/neutral invertase gene *DoNI* (Gao et al. 2016), the UDP-glucose pyrophosphorylase gene *DoUGP* (Wan et al. 2016), the phosphomannomutase gene *DoPMM* (He et al. 2017b), and eight cellulose synthase-like A genes *DoCSLA1-8* (He et al. 2015). In addition, our own research on *D. officinale* has revealed that WSPs are composed of mannose and glucose, forming parts of mannan polysaccharides, which accumulate in the stems of both juvenile and adult stages (He et al. 2015). Seeking to understand the relationship between UGE involved in the synthesis of WSPs and its abiotic stress tolerance, in this study, *DoUGE* from *D. officinale* was initially identified to illuminate the relationship between *DoUGE* and the biosynthesis of WSPs. The expression profiles of *DoUGE* and the content of WSPs in different organs and developmental stages of three cultivated varieties was explored by quantitative real-time PCR (qRT-PCR). Furthermore, transgenic *A. thaliana* lines overexpressing *DoUGE* were generated to clarify the association between the *DoUGE* gene and WSP synthesis. The tolerance of these lines to salt and osmotic stresses was also assessed. The important roles of *DoUGE* in the accumulation of WSPs and enhanced tolerance to salt and osmotic stresses are discussed.

Materials and methods

Plant materials, sampling and growth conditions

Dendrobium officinale seeds derived from selfing were germinated and cultured on half-strength Murashige

and Skoog medium (MS) (Murashige and Skoog 1962) under the same conditions as described previously by our research group (Zhang et al. 2016b). After germinating for 10 months in vitro, seedlings were collected. Adult plants obtained between 4 and 16 months after seedlings formed were transplanted into plastic pots and grown in a greenhouse at the South China Botanical Garden, Chinese Academy of Sciences, Guangzhou, China. To explore *DoUGE* in response to abiotic stresses and plant hormones, seedlings were subjected to half-strength MS containing 15% PEG, 250 mM NaCl, or 50 μM salicylic acid (SA) for 0, 4 and 12 h. In order to study the tissue-specific expression profiles of *DoUGE*, seedlings (roots, stems and leaves, 10 months after germinating) and adult plants [roots, stems, leaves, and flowers, 14 months after transplantation (MAT)] were excised. Four developmental stages in stems of *D. officinale*, S1 (4 MAT), S2 (8 MAT), S3 (12 MAT), and S4 (16 MAT), were sequentially harvested every quarter to focus on the spatial–temporal expression profiles of *DoUGE*. Stems of three genotypes (T10, T32-5 and T636) were collected at S1 to S4 to study the genotypic expression patterns. Each sample analysis used 30 strains of each genotype and each stage, with three independent replicates (i.e., 90 strains in total). 10 g of all collected samples were wrapped in tinfoil, frozen in liquid nitrogen, and then immediately transported to a −80 °C refrigerator until use for RNA extraction. The remaining sections were dried to a constant weight with a hot air-drying oven (Dongguan Haida Equipment Co., Guangzhou, China), weighed and ground into samples with a diameter less than 0.3 mm. This process was used to determine the contents and constituents of WSPs in *D. officinale*.

DoUGE overexpression lines and wild type (WT) *A. thaliana* (ecotype Columbia) were cultured in plastic pots (8 cm diameter and 6 cm height) filled with topsoil and vermiculite (1:2, v/v) in a growth chamber (day/night temperature: 22/16 °C; photoperiod: 16-h; relative humidity: 50%; photosynthetic photon flux density (PPFD): 40 μmol m^{-2} s^{-1}). Plants were regularly watered with 1.0 g l^{-1} Hyponex nutrient solution (Murakami Bussan Co., Kamigori, Japan). After measuring the chlorophyll content of three different leaf blades on at least three points on each blade using a SPAD-502 chlorophyll meter (Konica Minolta, Tokyo, Japan) as described previously (Ling et al. 2011), the leaves and stems of WT and transgenic *A. thaliana* plants were collected when plants were 30 days old. A fine *A. thaliana* powder was obtained as described above for *D. officinale*. All the above assays were carried out at least three times (≥ 3 replicates). Data was expressed as the average of three independent experiments.

Full-length cDNA cloning of *DoUGE* from *D. officinale*

Total RNA was isolated from *D. officinale* stems at 14 MAT in May with Column Plant RNAout2.0 (Tiandz, Inc., Beijing, China) following the manufacturer's instructions, and first-strand cDNA was reverse transcribed using a Reverse Transcriptase M-MLV Kit (Promega, Madison, WI, USA). A homology search for annotated unigenes in our transcriptome database (Zhang et al. 2016b) was used to design the *DoUGE* primers with Primer Premier 5.0 software (Premier Biosoft International, Palo Alto, CA, USA). The partial core fragments (476 bp) were cloned using TaKaRa LA Taq® (Takara Bio Inc., Dalian, China) according to the manufacturer's protocol. PCR products were subcloned with the pMD18-T vector (Takara Bio Inc., Dalian, China) and sequenced by the Beijing Genomics Institute (Shenzhen, China). The SMARTer RACE cDNA Amplification Kit (Clontech Laboratories Inc., Palo Alto, CA, USA) was used to amplify the complete 3′-UTR and 5′-UTR in accordance with the manufacturer's instructions. Four other gene-specific primers (GSPs) were used for 3′- and 5′-RACE (Supplementary Table S1).

Bioinformatics analysis of *DoUGE*

The open reading frame (ORF) of DoUGE as well as its functional domain were mined at NCBI (http://www.ncbi.nlm.nih.gov). The deduced proteins, molecular mass and theoretical isoelectric point of DoUGE were calculated by ExPASy (http://web.expasy.org/protparam). The putative amino acid sequence of DoUGE was compared with its counterparts in other organisms by running the ClustalX program (Thompson et al. 1997). MEGA 6.06 (Lynnon Biosoft, Foster City, CA, USA) was used to construct a phylogenetic tree (Tamura et al. 2013) with the Neighbor-joining (NJ) method (Saitou and Nei 1987). The SignalP program was applied to predict the signal peptide targeting location of the deduced amino acid sequences (http://www.cbs.dtu.dk/services/SignalP), while the transmembrane domains of the deduced proteins were identified by TMHMM (http://www.cbs.dtu.dk/services/TMHMM/). The predicted topology of DoUGE was determined by the TMpred program from Swiss EMBnet node (http://www.ch.embnet.org/software/TMPRED_form.html). The secondary structure of deduced DoUGE proteins was determined using the SOPMA program (http://npsa-pbil.ibcp.fr/). The SWISS-MODEL server (http://swissmodel.expasy.org) was applied to model the protein 3D conformation. In addition, the structural features of some catalytic active sites in DoUGE were confirmed using ProtScale (http://web.expasy.org/protscale/), NetNGlyc (http://www.cbs.dtu.dk/services/NetNGlyc/), NetPhos (http://www.cbs.dtu.dk/services/NetPhos/) and YinOYang (http://www.cbs.dtu.dk/services/YinOYang/).

Subcellular localization of DoUGE

A full-length *DoUGE* ORF, including the initiation codon but excluding the stop codon, was cloned with the Premix HS PrimeSTAR HS DNA Polymerase kit (Takara Bio Inc.) using primers YFPF/YFPR (Supplementary Table S1) and recombined into the *Nco*I site of pSAT6-EYFP-N1 plasmid (Citovsky et al. 2006) with the In-Fusion® HD Cloning Kit (Takara Bio Inc., Dalian, China) by replacing the DNA fragment encoding kanamycin resistance, downstream of the *Cauliflower mosaic virus* (CaMV) 35S promoter and in frame with the C-terminal enhanced yellow fluorescence protein (YFP) tag (Miyawaki et al. 1997). The recombinant vector obtained was analyzed and verified after full sequencing at the Beijing Genomics Institute. Mesophyll protoplasts were isolated using the Tape-*Arabidopsis* Sandwich method (Wu et al. 2009), and used to construct *35S::DoUGE-YFP* as in previous research (Yoo et al. 2007). YFP fluorescence was observed on a Zeiss LSM 510 confocal microscope (Carl Zeiss, Jena, Germany).

Molecular cloning and analysis of the putative promoter of *DoUGE*

The putative *DoUGE* promoter was cloned by a thermal asymmetric interlaced polymerase chain reaction using primers AD1-3/Tail1-3 (Supplementary Table S1) as previously described (Michiels et al. 2003). Tertiary PCR products (1200 bp) were purified, cloned into the pMD18-T vector and sequenced as described above. Putative *cis*-regulatory elements of the *DoUGE* promoter were identified against the PlantCare database (http://bioinformatics.psb.ugent.be/webtools/plantcare/html/).

Quantitative real-time PCR analysis of *DoUGE* in *D. officinale*

cDNA used for qRT-PCR was prepared from *D. officinale* as described above. The qRT-PCR assay was performed on an ABI 7500 Real-time system (ABI, Foster City, CA, USA), and in 10 µl of reaction containing 1 × SYBR Premix Ex Taq™ (Takara Bio Inc., Kyoto, Japan), 10 µM solution of each primer, and 100 ng of cDNA. Thermocycling conditions were: initial denaturation at 95 °C for 2 min, followed by 40 cycles of 15 s at 95 °C and 1 min at 60 °C. The relative expression of *DoUGE* was assessed by the comparative threshold cycle (Ct) method (Schmittgen and Livak 2008). The *D. officinale* actin gene (JX294908) served as an internal control for signal normalization. Expression levels were evaluated as technical duplicates of biological triplicates.

Construction of *DoUGE* overexpression vector and its transformation into *A. thaliana*

For overexpression constructs, the coding sequence of the *DoUGE* gene (including the initiation codon but without the stop codon) was cloned into the plant-based expression vector pCABIA 1302 at the *Nco*I site with the In-Fusion® HD Cloning Kit (Takara Bio Inc., Dalian, China), under the control of a CaMV 35S promoter. After checking the recombinant plasmid via complete Sanger sequencing at the Beijing Genomics Institute, it was transferred into *A. tumefaciens* EHA105 (Biovector Science Lab, Inc. Beijing, China) using the freeze–thaw method (Jyothishwaran et al. 2007), and then introduced into *A. thaliana* by the floral-dip method (Clough and Bent 1998). Harvested transgenic seeds were plated on half-strength MS medium supplemented with 50 µg ml^{-1} hygromycin, which was applied to identify transformed seedlings as described by Harrison et al. (2006), and then reevaluated by semi qRT-PCR. The primers designed for *35S::DoUGE* are described in Supplementary Table S1.

Semi-quantitative RT-PCR

For semi qRT-PCR, total RNA was extracted from WT and transgenic *A. thaliana* lines as described previously (He et al. 2017b). Verification of *DoUGE* levels followed a previously described method (He et al. 2015) by using a LabCycler thermal cycler (Sensoquest, Hannah, Germany). The primers for ubiquitin (AtUBQ10, AT4G05320) are shown in Supplementary Table S1.

Determination of UGE activity in *A. thaliana* seedlings

The UGE activity assay was identical to that previously described by Rosti et al. (2007). Quantification of UGE activity in *A. thaliana* and *D. officinale* plant cells were carried out at 340 nm in an UV-6000 spectrophotometer (Shanghai Metash Instruments Co., Shanghai, China), and expressed as U g^{-1} protein.

Analysis of stress tolerance in transgenic *A. thaliana* seedlings

To examine salt and osmotic stress tolerance, independent homozygous line 1, 2 and 3 containing and overexpressing *DoUGE* in the T_3 generation were subjected to salt and osmotic stress. The seeds were surface-sterilized as described in Zhang et al. (2006), and then germinated on half-strength MS medium in the same growth chamber as indicated above after a 2-day stratification period at 4 °C in the dark. For the growth assay, 7-day-old seedlings of WT and *35S::DoUGE* transgenic *A. thaliana* were transferred to fresh half-strength MS medium supplemented with either

150 mM NaCl as salt stress or 200 mM mannitol as drought stress based on Tamirisa et al. (2014). After 5 days, average root length and fresh weight were estimated. Free proline content and malondialdehyde (MDA) were estimated following Zhang et al. (2012). MDA was expressed in μmol g^{-1} FW while proline content was expressed as mg g^{-1} FW. NaCl and mannitol treatments were repeated three times, and ten plants were collected in each assay.

Quantification of water-soluble polysaccharides and their composition

WSPs in the stems of *D. officinale* and in *A. thaliana* seedlings were extracted using a SXT-06 Soxhlet extractor (Hangzhou Chincan Trading Co., Hangzhou, China) as described by He et al. (2015). WSPs were quantified in each 200 μl fraction using the phenol–sulfuric acid method (Dubois et al. 1956). The composition of monosaccharides in WSPs in the above-ground organs of *A. thaliana* was assessed using a previous report (Li et al. 2014) and determined by High Performance Liquid Chromatography (HPLC; Agilent 1100, Agilent Technologies Inc., Santa Clara, CA, USA) on an Ultimate® XB-C18 column (4.6 × 250 mm, 5 μm) using a mixture of 17% acetonitrile and 83% (v/v) 0.02 M ammonium acetate as the eluent (1.0 ml min^{-1}). All experiments were repeated in triplicate.

Statistical analysis

Statistical analyses were performed using IBM SPSS Statistics version 22.0 for Windows (IBM Corp., Armonk, NY, USA). Significant differences among tissues, stages, genotypes and lines were assessed by Duncan's multiple range test ($p < 0.05$). Correlations among the accumulation of WSPs, DoUGE activity and *DoUGE* expression were calculated using Pearson's correlation coefficient (R^2; $p < 0.01$). For different *D. officinale* genotypes and different *A. thaliana* transgenic lines, the *DoUGE* transcript levels and the content of WSPs were analyzed. Graphs in this study were plotted in Sigmaplot 12.5 (Systat Software Inc., San Jose, CA, USA).

Results

Molecular cloning and bioinformatics analysis of *DoUGE* from *D. officinale*

DoUGE, which encodes UDP-glucose 4-epimerase, was cloned from *D. officinale* for the first time. Sequence analysis of *DoUGE* indicated that the full-length cDNA was 1791 bp (GenBank accession number: KX545406) including a 221 bp 5′-untranslated region, a 1254 bp ORF and a 316 bp 3′-untranslated region (Fig. 1a, Supplementary Txt. S1). The deduced DoUGE nucleotides encode 417 amino acids with a predicted molecular mass of 46.6 kD and an isoelectric point of 9.37. Searching against the CDD revealed that DoUGE contains the UDP_G4E_1_SDR_e domain (position 72–403), which belongs to the DADB_Rossmann superfamily (Fig. 1b). The predicted secondary structure of DoUGE consists of 36.93% alpha helices, 34.53% random coils, 18.94% extended strands and 9.59% beta turns (Fig. 1c). The tertiary structure of DoUGE is shown in Fig. 1d.

TMHMM analysis indicated that DoUGE includes a transmembrane domain at residues 33–51 (Supplementary Fig. S1). The TMpred analysis suggested that DoUGE has three possible transmembrane helices situated at positions 38–57, 73–93 and 146–164 from the inside to the outside (Supplementary Fig. S2). No signal peptide was identified by SignalP software (Supplementary Fig. S3). NetNGlyc analysis revealed that two *N*-glycosylation sites were identified at positions 102 and 171 (Supplementary Fig. S4). DoUGE phosphorylation sites were predicted as follows: 18 serine, 18 threonine and seven tyrosine (Supplementary Fig. S5). There was an *O*-glycosylation site in DoUGE (Supplementary Fig. S6). A minimum value of −2.856 and a maximum value of 3.722 were found using ProtScale, indicating that DoUGE might be a hydrophilic protein (Supplementary Fig. S7).

Localization of DoUGE using YFP tagging

The subcellular localization of UGE from *Aspergillus nidulans* was cytoplasmic (El-Ganiny et al. 2010). In addition, UGE1, UGE2, and UGE4 from *A. thaliana* were localized in the cytoplasm (Barber et al. 2006). Confocal microscopy experiments showed that DoUGE protein was localized in the cytoplasm (Supplementary Fig. S8). Most UGEs isolated from plants appear to be stored as soluble entities in the cytoplasm, as they lack transmembrane motifs and signal peptides (Li et al. 2011).

Homology and phylogenetic analysis of DoUGE

The NJ method showed that distances between different genera were relatively large, while those within genera were relatively small (Lu et al. 2014). Phylogenetic analysis suggested that DoUGE is evolutionarily closer to monocotyledonous plants such as *Oryza sativa* and *Brachypodium distachyon* than to three dicotyledonous plants, *A. thaliana, Glycine max* and *Nicotiana tabacum* (Fig. 2). Multi-alignment by ClustalX showed that DoUGE is phylogenetically closer to *Elaeis guineensis* and *Phoenix dactylifera*. Phylogenetic trees of *D. officinale* protein DoUGE with other plants were divided into two classes, and the tree that contained DoUGE was chosen for further homology analysis.

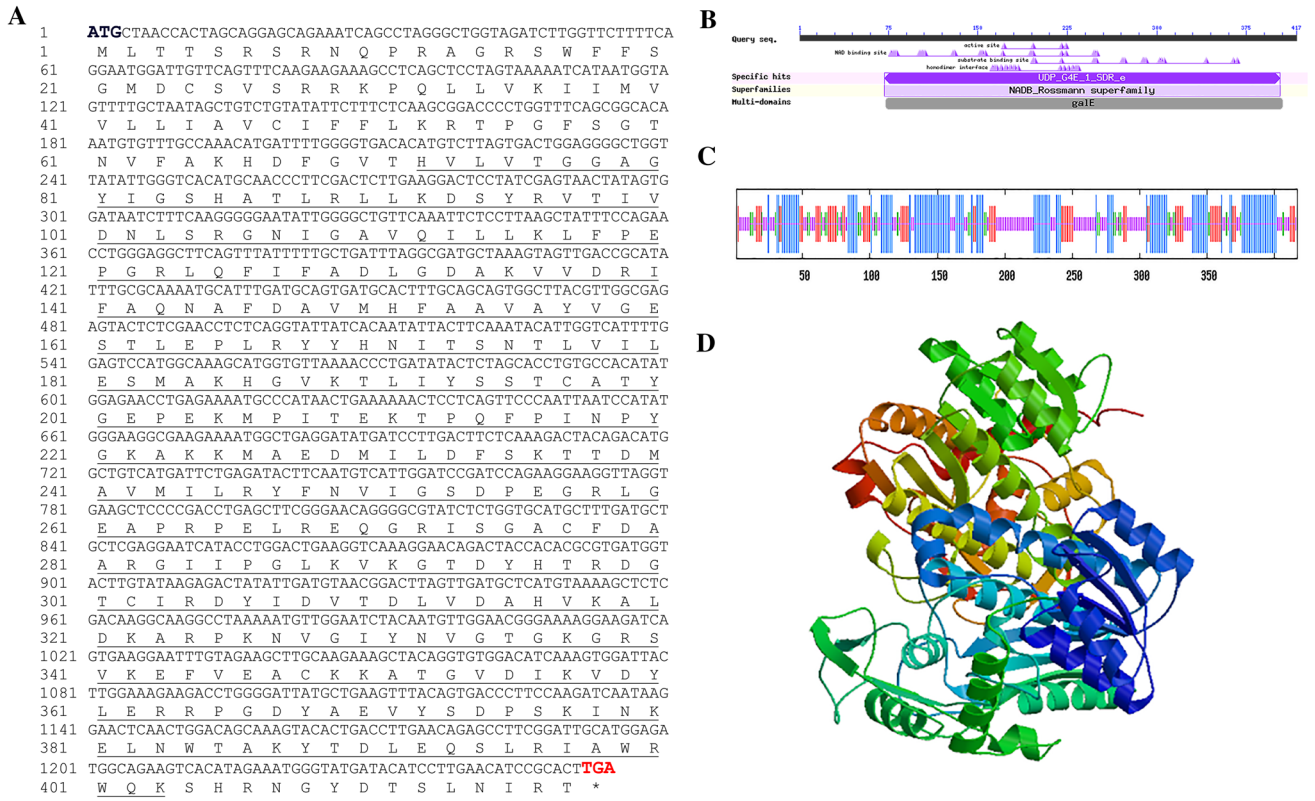

Fig. 1 Sequence analysis of *DoUGE*. **a** Coding sequences and their deduced amino acid sequences. The start codon is shown in blue, the termination codon is shown in red, and the domain of the short-chain dehydrogenase/reductase (SDR) superfamily is underlined. **b** Functional domains are found at NCBI (https://www.ncbi.nlm.nih.gov/). **c** Secondary structures. The alpha helix is indicated by the longest vertical bar, the extended strand is indicated by the second longest vertical bar, the random coil is indicated by the third longest vertical bar, and the beta turn is indicated by the shortest vertical bar. **d** The tertiary structure of DoUGE was assessed using SWISS MODEL (http://swissmodel.expasy.org). (Color figure online)

The amino acid sequences of DoUGE were aligned with known amino acid sequences of their counterparts in other plant species using DNAMAN (Fig. 3). Homology analyses indicated that DoUGE shared 82.5, 75.5, 79.0, 83.0, 78.5, 82.5, 80.2 and 79.1% sequence similarity with *Elaeis guineensis, Glycine max, Brachypodium distachyon, Musa acuminata, Oryza sativa, Phoenix dactylifera, Sorghum bicolor* and *Zea mays*, respectively. The percentage identity and similarity of the query with these sequences showed that DoUGE was closely related to UGE proteins in *Musa acuminata* and *Phoenix dactylifera*.

Indeed, different UGE isoforms in the same family could play different roles. For instance, five UGE genes from *A. thaliana* (AtUGE1-5; Barber et al. 2006), as well as four UGE genes from *O. sativa* (OsUGE1-4; Kim et al. 2009), made different contributions to carbohydrate metabolism, biomass accumulation and stress response. In order to estimate the number of UGE isoforms in *D. officinale*, a transcriptome-wide investigation was applied. After searching all 145,791 unigenes in our transcriptome database (NCBI accession number: SRR1904494 and SRR1909493; Zhang et al. 2016b) against COG, GO, KEGG, Swissprot and Nr database, 22 unigenes were annotated as 'UDP-glucose 4-epimerase' (Supplemental Table S2). In order to remove stitching errors and redundant fragments, all chosen unigenes were further confirmed with BLAST searches against the NCBI database. Furthermore, the genetic distance was the fixation index that ranged from 0 to 1 among different unigenes, while any value greater than 1 was abandoned. Thus, nine UGE unigenes from *D. officinale* were finally selected. A molecular phylogenetic tree of the UGE family of *A. thaliana, O. sativa* and nine UGE unigenes from *D. officinale* was constructed using the NJ method, resulting in the formation of six clusters. Interestingly, these nine UGE unigenes were divided into four clusters (A, B, C and D, Supplemental Fig. S9). Unigene0026017, Unigene0131022 and Unigene0131020 were placed into cluster A, Unigene0059580 was included in cluster B, DoUGE, Unigene0024806 and Unigene0143087 were grouped into cluster C, while Unigene0100277, Unigene0100904 and Unigene0124811 were placed into cluster D. Therefore, four UGE isoforms were found in *D. officinale*, which was

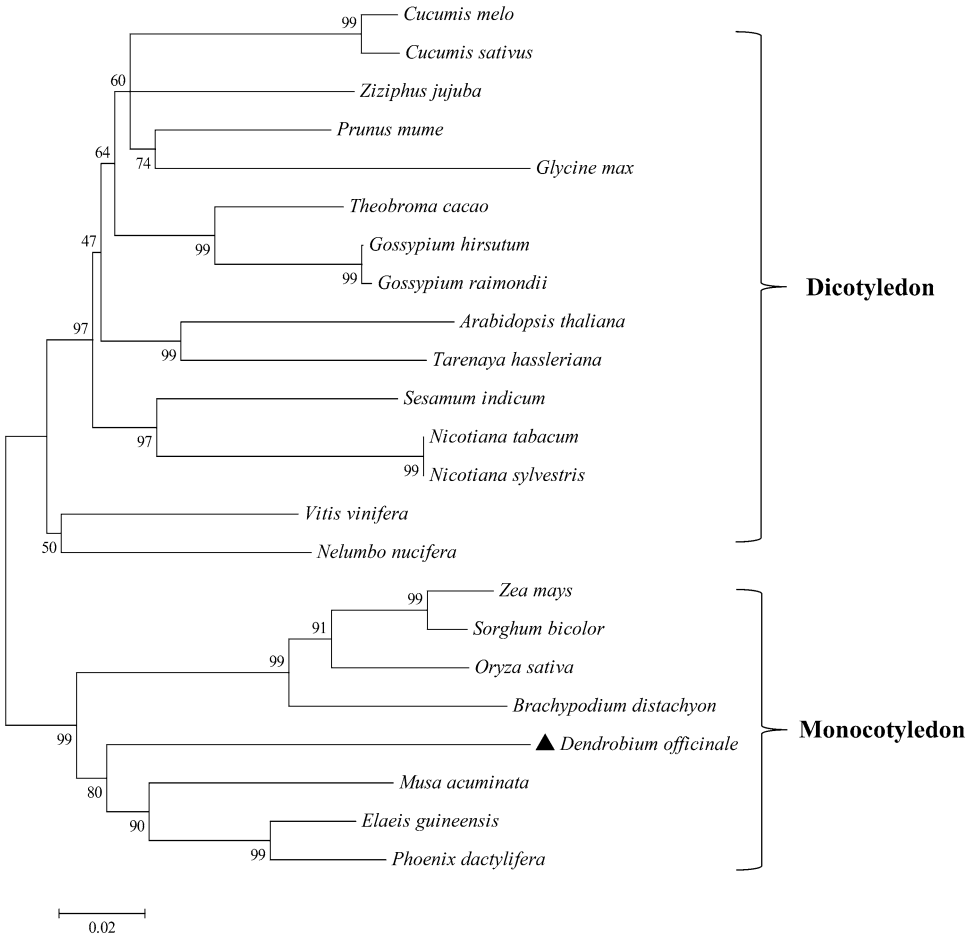

Fig. 2 Molecular phylogenetic trees of DoUGE from *D. officinale* with UGEs from other plants constructed by the neighbor-joining method using MEGA 6.06 software. Values at branch-points represent percentage frequencies for tree topology after 1000 iterations. UGE proteins used for phylogenetic profiling alignment are as follows: *Oryza sativa* (BAC53786.1), *Arabidopsis thaliana* (AAN60309.1), *Glycine max* (XP_003531307.1), *Zea mays* (XP_008658853.1), *Elaeis guineensis* (XP_010941587.1), *Phoenix dactylifera* (XP_008808530.1), *Gossypium hirsutum* (XP_016754266.1), *Brachypodium distachyon* (XP_003573339.1), *Sorghum bicolor* (XP_002468003.1), *Nicotiana tabacum* (XP_016477501.1), *Ziziphus jujube* (XP_015900710.1), *Theobroma cacao* (XP_007022982.1), *Nelumbo nucifera* (XP_010258705.1), *Sesamum indicum* (XP_011096743.1), *Gossypium raimondii* (XP_012451226.1), *Nicotiana sylvestris* (XP_009783848.1), *Tarenaya hassleriana* (XP_010540637.1), *Prunus mume* (XP_008225692.1), *Vitis vinifera* (XP_010655780.1), *Cucumis melo* (XP_016902341.1), *Musa acuminata* (XP_009385042.1), and *Cucumis sativus* (XP_004135561.1)

phylogenetically closer to a monocotyledonous plant, *O. sativa*.

Identification of *cis*-elements in *DoUGE* promoter regions and their expression profiles under PEG, NaCl and SA treatments

Cis-acting elements play critical roles in determining the organ-specific or stress-responsive expression profiles of gene promoter regions (Walther et al. 2007). Here, various *cis*-regulatory elements were widespread in 2000-bp putative promoter regions of *DoUGE* (Fig. 4, Supplementary Txt. S2), including a TCA-element involved in salicylic acid responsiveness (Bari and Jones 2009), the MYB-binding site (MBS) and the CCAAT-box (MYBHv1 binding site), which are well-known *cis*-acting regulatory elements involved in drought response (Dubos et al. 2010), and two TC-rich repeats involved in defense and stress responsiveness (Diaz de Leon et al. 1993). In addition, light-responsive elements and multi-stimulus responsive elements, such as a GATA-motif, a GARE-motif, and a TGA-element, were also found. The details of these findings, which are shown in Supplementary Table S3, would allow the further exploration of possible stress-responsive mechanisms in *D. officinale*. Hence, the relative mRNA level of *DoUGE* in NaCl (250 mM), PEG (15%, m/v), or SA (50 mM) was investigated (Fig. 5). *DoUGE* was obviously up-regulated in all treatments ($p < 0.05$),

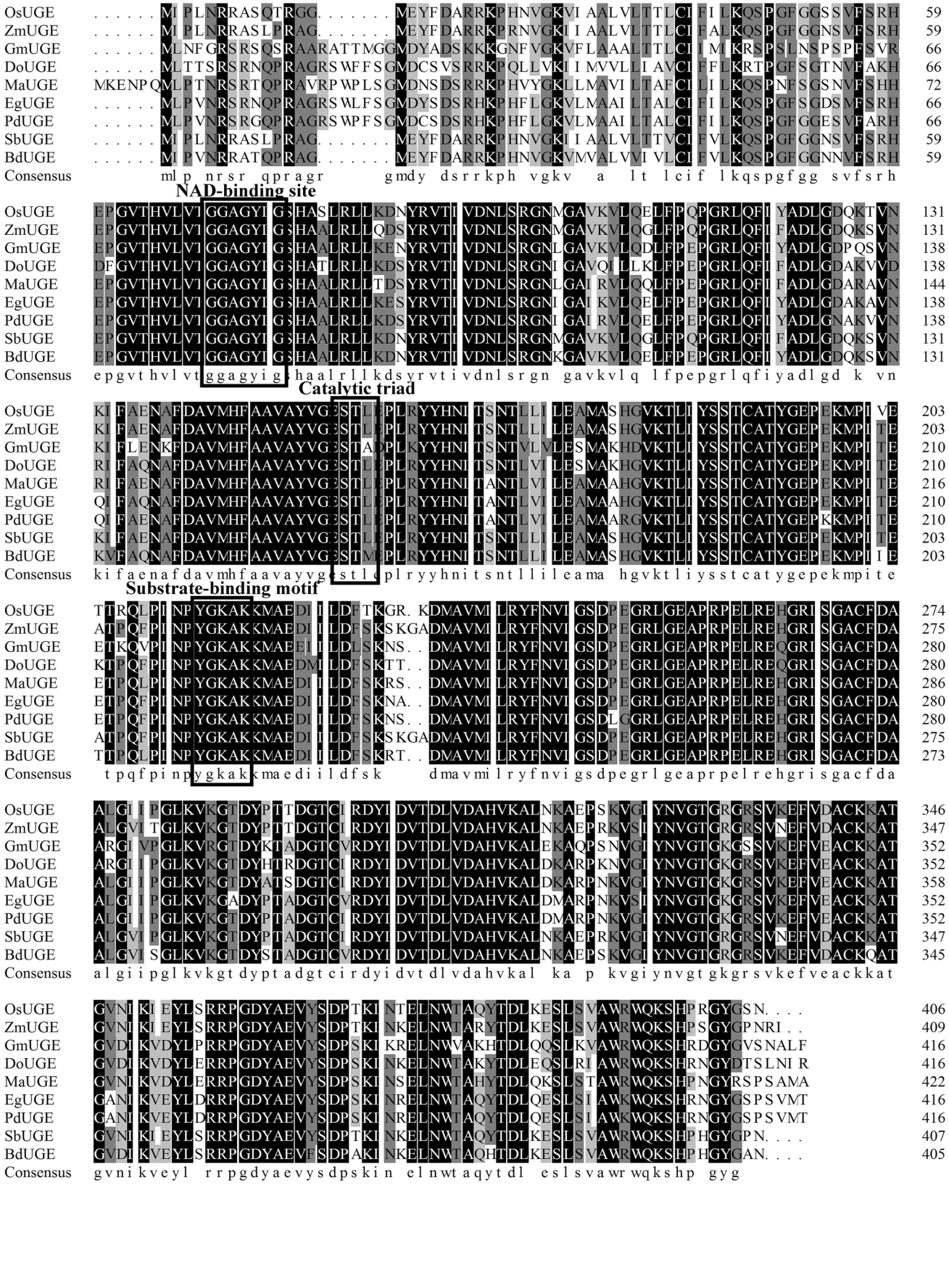
NAD-binding site
Catalytic triad
Substrate-binding motif
OsUGE
ZmUGE
GmUGE
DoUGE
MaUGE
EgUGE
PdUGE
SbUGE
BdUGE
Consensus

◂**Fig. 3** Multiple alignment of DoUGE with known UGEs of other plants using the ClustalX2 multiple alignment tool. The conserved NAD-binding motif (GxxGxxG), catalytic amino acid residues Ser and tyrosine substrate-binding motif (YxxxK) are underlined. UGE proteins used for alignment are as follows: OsUGE (BAC53786.1), ZmUGE (XP_008658853.1), GmUGE (XP_003531307.1), MaUGE (XP_009385042.1), EgUGE (XP_010941587.1), PdUGE (XP_008808530.1), SbUGE (XP_002468003.1) and BdUGE (XP_003573339.1), which represent UGE proteins from *Oryza sativa, Zea mays, Glycine max, Musa acuminata, Elaeis guineensis, Phoenix dactylifera, Sorghum bicolor* and *Brachypodium distachyon*, respectively

indicating that *DoUGE* played a vital role in regulating stress responses in *D. officinale*, resulting from stress-inducible elements in *DoUGE* promoter regions.

Organ-specific expression patterns of *DoUGE* in *D. officinale*

In a monocotyledonous model plant, *OsUGE*1-4 were expressed in various tissues of *O. sativa*, with a higher expression level of *OsUGE3* in leaves, seeds and roots relative to the stems, while highest *OsUGE4* expression was in stems (Kim et al. 2009). To determine tissue-specific expression patterns of *DoUGE* in *D. officinale*, qRT-PCR was used to analyze the expression levels of seedlings (including roots, stems and leaves) and adult plants (including roots, stems, leaves and flowers) (Fig. 6). Whether in seedlings or in adult plants, *DoUGE* was constitutively expressed in the roots, stems, leaves and flowers of *D. officinale*, while *DoUGE* transcript levels demonstrated a tissue-specific expression pattern. In seedlings, *DoUGE* showed high transcript levels in stems (Fig. 6a). In adult plants, higher expression levels of *DoUGE* were observed in stems and flowers than in roots and leaves, but especially in stems (Fig. 6b), mainly because *D. officinale* stems are the principal storage organs for WSPs (He et al. 2017a).

Analysis of WSPs in *D. officinale* at different developmental stages

In our previous study, WSP had been demonstrated to exist in all tissues, but particularly bio-accumulated in stems while the content of WSPs changed during different developmental periods (He et al. 2015). In this study, the content of WSPs in *D. officinale* stems was detected quarterly at different developmental stages (Fig. 7a). The content of WSPs ranged from 186.43 to 412.16 mg g^{-1} DW during S1 to S4, with an average value of 309.38 mg g^{-1} DW. Along with the growth process, the changes in WSPs of *D. officinale* followed an S-shaped curve. The highest WSP content was detected in S3, and the lowest in S1.

Expression levels of *DoUGE* in *D. officinale* at different developmental stages

To understand the spatial–temporal expression profiles, a detailed expression analysis of *DoUGE* focused on the stems of *D. officinale* during the four developmental stages (S1–S4, Fig. 7b). *DoUGE* expression increased at first, then decreased and possessed the highest value in S3, corresponding to a gradual increase and then a decrease in the content of WSP at the same developmental stage (Fig. 7a).

Analysis of WSPs in different cultivated varieties of *D. officinale*

Plant genotype and habitat environment are the most important factors when determining the content of polysaccharides in *D. officinale* (Yun et al. 2015; Jin et al. 2016). In this study, WSPs were detected in three cultivated varieties (T10, T32-5 and T636), showing a significant difference in content among them, ranging from 175.88 to 427.86 mg g^{-1} DW during the four developmental stages (S1 to S4), with an average value of 306.72 mg g^{-1} DW (Fig. 8a). The differences in WSPs among *D. officinale* varieties is in agreement with previous findings (Zhu et al. 2010). The highest average level of WSPs was found in T636, while the lowest was observed in T10. Furthermore, the WSP content in T10, T32-5 and T636 followed an S-shaped, but uneven, curve from S1 to S4. This trend confirmed previous observations (Zhu et al. 2010; He et al. 2015).

The expression levels of *DoUGE* in different cultivated varieties of *D. officinale*

Given the differences of WSPs among different cultivated varieties and at different developmental stages (Fig. 8a), it was crucial to investigate the expression patterns of *DoUGE* in *D. officinale* (Fig. 8b). The expression of *DoUGE* in all three cultivated varieties increased at first, then decreased as the developmental period was extended, while the highest level of *DoUGE* expression was detected in S3. In addition, the *DoUGE* transcript levels were strongly correlated with the change in content of WSPs ($R^2 = 0.98$, $p < 0.01$).

Qualification of DoUGE activity in *D. officinale*

To clarify the correlation among DoUGE activity, *DoUGE* expression and WSP content, DoUGE activity was monitored in four *D. officinale* genotypes (T6, T10, T32-5 and T636) during four developmental periods (S1 to S4, Supplementary Fig. S10). Similar patterns were observed in T6, T10, T32-5 and T636, ranging from 23.35 to 36.73 U g^{-1} protein, with the lowest in S1, higher in S2, peaking in S3, and low in S4. Furthermore, *DoUGE* transcript levels were

```
+ TACATATAGA AGAATAGAAG TTGGCATTGT TGAAAGAAGA ACAACTAAAA GATTTGACTA CTAACATCCA
- ATGTATATCT TCTTATCTTC AACCGTAACA ACTTTCTTCT TGTTGATTTT CTAAACTGAT GATTGTAGGT

+ AATATTAAAG TTAAGATTGC AAGAGATTTC ACCATTTTTG GAGACCGGTT TCCTTGGTGG GCAGGCTATA
- TTATAATTTC AATTCTAACG TTCTCTAAAG TGGTAAAAAC CTCTGGCCAA AGGAACCACC CGTCCGATAT

+ GAAACAATTT ATCTTGAATA GCTTGAGAAG TCGAGAGCTC CTCTTTGGAT AGTTGTCACC CGTAGGTTGA
- CTTTGTTAAA TAGAACTTAT CGAACTCTTC AGCTCTCGAG GAGAAACCTA TCAACAGTGG GCATCCAACT

+ GCGTGTATAA TATTTGTAGT ATTAGATAGG AGAAATTAAG CTGAGGAATG GAGATTTCTC CCATTTTGAT
- CGCACATATT ATAAACATCA TAATCTATCC TCTTTAATTC GACTCCTTAC CTCTAAAGAG GGTAAAACTA

+ AATGGAATTG TATTCAACTT GATGAGAGTT CCTGGACGAT CATGAGGAGC AGAGTACCAG AAGGAAAGTT
- TTACCTTAAC ATAAGTTGAA CTACTCTCAA GGACCTGCTA GTACTCCTCG TCTCATGGTC TTCCTTTCAA

+ TAGAATTGAA TGCCGTTATA CAAAAGAAGT TTTGGTACCA TGAGGATTAC TGAAATAAAG AAAAAGAATA
- ATCTTAACTT ACGGCAATAT GTTTTCTTCA AAACCATGGT ACTCCTAATG ACTTTATTTC TTTTTCTTAT

+ TAACATAATA TAAAAGAGAA ACAAAGAAGA GTGCAAACCT TTATTTATTA AGCACAGCAG CTTCAGTTTT
- ATTGTATTAT ATTTTCTCTT TGTTTCTTCT CACGTTTGGA AATAAATAAT TCGTGTCGTC GAAGTCAAAA

+ TGACCAACGG CTGAGTAGCA GAGATGATTG ATTATAAGGG AATGGTGATC AGCAATAAGG ACGTAAATAT
- ACTGGTTGCC GACTCATCGT CTCTACTAAC TAATATTCCC TTACCACTAG TCGTTATTCC TGCATTTATA

+ ACAGAGAAAG TGGCTGCCAG ATTATTAGAG TGAATGGAAT TGATTTTGCA TTGTTATTTG TTAACAAAAA
- TGTCTCTTTC ACCGACGGTC TAATAATCTC ACTTACCTTA ACTAAAACGT AACAATAAAC AATTGTTTTT

+ GGGCAAATTT ACAGTTGCGT CTCTATTTGT ATATATATAT TTTTTGTTCG AGGACTTCCA GGTGGAAGTC
- CCCGTTTAAA TGTCAACGCA GAGATAAACA TATATATATA AAAAACAAGC TCCTGAAGGT CCACCTTCAG

+ AACATTGGAG AAAACGCTCG CAGGACGGCT AAAAGAAACT GAAGAAAAGG CAGAAAAAAG TCTTCTCCTT
- TTGTAACCTC TTTTGCGAGC GTCCTGCCGA TTTTCTTTGA CTTCTTTTCC GTCTTTTTTC AGAAGAGGAA

+ ACAAGGAACC AATCAAATGA ACATGGGAGG AGCGCCGAGA AGCCAGTCAG ATCCTAAAAA TTTCTCATTT
- TGTTCCTTGG TTAGTTTACT TGTACCCTCC TCGCGGCTCT TCGGTCAGTC TAGGATTTTT AAAGAGTAAA

+ CTTCGTTCTT TCTCTCATTT GTTCTCATTC CCCTATATTT GCACACTCCT CTCTCTGTTT TTCGCTTTCT
- GAAGCAAGAA AGAGAGTAAA CAAGAGTAAG GGGATATAAA CGTGTGAGGA GAGAGACAAA AAGCGAAAGA

+ CTTCAAACGC CTCGAAAAGG CGTCGACTTG ATCCAAAAGC TCCCAAATCC ACACATCTTT GTCGCTTGCG
- GAAGTTTGCG GAGCTTTTCC GCAGCTGAAC TAGGTTTTCG AGGGTTTAGG TGTGTAGAAA CAGCGAACGC

+ GTCTCTCCAA ACCTTTATAT CTCTTATCGC CGGTTTCGTC GCTGACTTTT GAAGTTTGGC GTCTCCCAAA
- CAGAGAGGTT TGGAAATATA GAGAATAGCG GCCAAAGCAG CGACTGAAAA CTTCAAACCG CAGAGGGTTT

+ CACAATAGCT TTGTTTCCAG ATAGGAGTCG TACTGTACTT TAGTTGGTGC AGAGTCGTTG AAAGATTCCG
- GTGTTATCGA AACAAAGGTC TATCCTCAGC ATGACATGAA ATCAACCACG TCTCAGCAAC TTTCTAAGGC

+ GTAATCAAAG AGAAGGAGCT TTCTTTTTGT TTTTTAATGG AGCAGTTTGT TTCTGCTTGA TTTCAGAGTA
- CATTAGTTTC TCTTCCTCGA AAGAAAAACA AAAAATTACC TCGTCAAACA AAGACGAACT AAAGTCTCAT

+ TTTCCTCA
- AAAGGAGT
```

CCAAT-box	GT1-motif	TCA-element
TGA-element	Gap-box	GARE-motif
TC-rich repeats	HSE	MBS
Box-W1	CAT-box	AE-box

◂**Fig. 4** Putative regulatory *cis*-elements in the *DoUGE* promoter. AE-box, part of a module for the light response; Box-W1, fungal elicitor responsive element; CAT-box, *cis*-acting regulatory element related to meristem expression; CCAAT-box, MYBHv1 binding site; Gap-box, part of a light responsive element; GARE-motif, gibberellin-responsive element; GT1-motif, light responsive element; HSE, *cis*-acting element involved in heat stress responsiveness; MBS, MYB binding site involved in drought-inducibility; TC-rich repeats, *cis*-acting element involved in defense and stress responsiveness; TCA-element, *cis*-acting element involved in salicylic acid responsiveness; TGA-element, auxin-responsive element. PLANTCARE (http://bioinformatics.psb.ugent.be/webtools/plantcare/html/) was used for the promoter analysis

almost perfectly correlated with DoUGE activity ($R^2 = 0.92$, $p < 0.01$) in different genotypes during the four developmental stages (Fig. 9).

Overexpression of *DoUGE* in *A. thaliana*

To understand the biological role of the *DoUGE* gene, the plasmid pCABIA 1302-*DoUGE* containing the *DoUGE* ORF driven by the CaMV-35S promoter was constructed (Fig. 10a). No obvious phenotypic differences between *35S::DoUGE* and WT were observed under normal conditions (Fig. 10b). Semi-quantitative RT-PCR analysis results confirmed that *DoUGE* was detected in the three homozygous transgenic lines (lines 1, 2 and 3) produced by self-pollination, and that no amplification was observed in WT (Fig. 10c). Further PCR analysis confirmed homozygous transformants in the T_3 generation (Fig. 10d), and these were chosen for subsequent experiments. Furthermore, with respect to WT, the chlorophyll content was slightly elevated (1.26-, 1.31-, 1.19-fold, respectively) in the transgenic lines (Fig. 10e). Previous research in *O. sativa* found that the *phd1* mutant, which encoded a chloroplast-localized UGE, demonstrated decreased chlorophyll content and photosynthetic activity, resulting in an increase in chlorophyll content (Li et al. 2011).

Analysis of water-soluble polysaccharides in *A. thaliana* transgenic lines

In a previous study, UGE catalyzed the inter-conversion between UDP-glucose and UDP-galactose, a process that is considered to be critical for the accumulation of polysaccharides (Niou et al. 2009). In order to further study the *DoUGE* related to WSPs in transgenic *A. thaliana*, the above-ground parts of 1-month-old WT and transgenic lines were harvested. UGE activity in three confirmed lines with *DoUGE* overexpression was significantly higher than in WT (Fig. 11a), which was consistent with the transcription of *DoUGE*. Analysis of WSPs revealed that transgenic lines outperformed WT, showing significantly (1.35-, 1.45-, 1.38-fold in lines 1, 2 and 3, respectively) higher levels than WT (Fig. 11b). In a parallel experiment, the composition of WSPs containing glucose, mannose, and galactose in WT and *35S::DoUGE* transgenic lines was investigated using a pre-column PMP derivatization HPLC method (Fig. 11c). The glucose content improved significantly in three transgenic plants compared with WT, while significant increases in galactose were also detected. However, no significant change in mannose levels was observed between transgenic lines and WT. This is because mannose is derived from GDP-mannose (Reiter and Vanzin 2001) while UGE is responsible for the freely reversible interconversion between UDP-glucose and UDP-galactose in planta (Dormann and Benning 1998).

In addition, the *DoUGE* expression levels in transformants were significantly positively correlated with the content of WSPs ($R^2 = 0.89$, $p < 0.01$). Until now, WSPs isolated from *D. officinale* are mannan polysaccharides (Xing et al. 2013). Given the proposed biosynthetic pathway of WSPs (Supplementary Fig. S11), the expression profiles of several genes associated with WSP in *A. thaliana* were observed. The expression of *AtSUS, AtINV, AtCslA1* and *AtCslA9* showed a dramatic increase in *35S::DoUGE* transgenic lines compared to WT plants (Fig. 12). This led to a large increase in the production of WSPs (Fig. 11b).

The physiological role of *DoUGE* in salt and osmotic stress tolerance

Recent studies revealed that the overexpression of *BrUGE1* in *A. thaliana* improved agronomic traits, which led to obviously increased tolerance against drought stress (Abdula et al. 2016). To better analyze the potential role of *DoUGE* in response to abiotic stress in *A. thaliana*, WT and transgenic plants were grown in separate media containing NaCl (150 mM) as the salt stress, and mannitol (200 mM) as the osmotic stress. No difference in germination was observed between transgenic and control plants under normal conditions (Supplementary Fig. S12), nor were there any significant differences in root length and fresh weight between *DoUGE* transgenic lines and WT in medium at 1 week after stratification without NaCl and mannitol (Fig. 13). However, the root length of transgenic lines 1, 2 and 3 increased significantly by 35.12, 44.33, and 38.97%, respectively compared with WT under 150 mM NaCl stress (Fig. 13a). Transgenic lines 1, 2 and 3 of *A. thaliana* seedlings accumulated significantly more fresh weight (1.37-, 1.45-, and 1.38-fold, respectively) than WT (Fig. 13b). Similarly, growth parameters including root length and fresh weight in transgenic lines 1, 2 and 3, when compared with WT, were significantly improved on half-strength MS medium supplemented with 200 mM mannitol (Fig. 13). Furthermore, the MDA and proline contents, which are important indicators of osmotic stress tolerance, were statistically similar under control

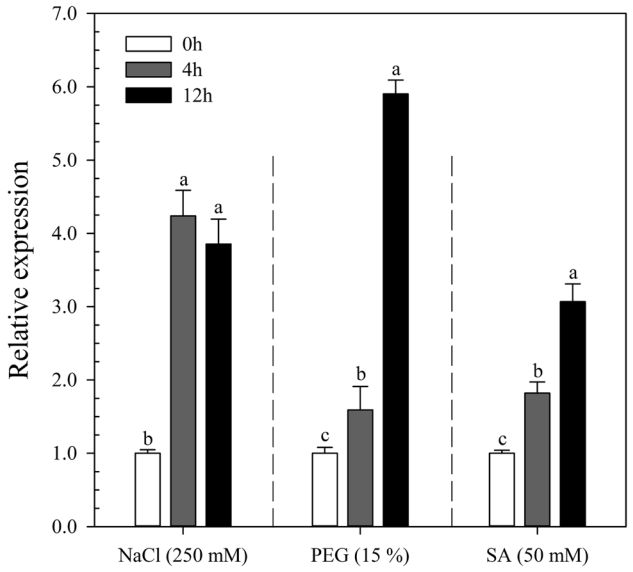

Fig. 5 Abundance of transcripts in *D. officinale* exposed to various stresses. Seedlings about 10 months after germination were subjected to drought stress (PEG), salt stress (NaCl) and salicylic acid (SA). Error bars indicate the mean ± standard deviation of three biological replicates. Different letters above bars indicate significant differences by Duncan's multiple range test ($p < 0.05$)

conditions (Fig. 14). The *A. thaliana* seedlings under salt stress showed enhanced MDA and proline accumulation (the enhancement was greater for MDA than for proline), and transgenic lines showed significantly lower MDA and proline contents than WT (Fig. 14). Likewise, the contents of MDA and proline in transgenic plants were higher than in the control group, but lower than WT levels under drought stress. These results suggest that the *DoUGE* gene enhanced tolerance to salt and osmotic stress.

Discussion

Structural analysis of *Do*UGE in *D. officinale*

UGE catalyzes the reversible interconversion of UDP-glucose and UDP-galactose, which are critical precursors for the synthesis of soluble sugars, hemicellulose and cellulose (Majumdar et al. 2004). In this study, the full-length cDNA of *DoUGE* was cloned from *D. officinale* for the first time (Fig. 1). Four UGE isoforms was found in *D. officinale* based on a transcriptome-wide investigation (Supplemental Table S3). DoUGE was phylogenetically closer to monocotyledonous plants, especially *Phoenix dactylifera* and *Elaeis guineensis*, then to dicotyledonous plants (Fig. 2). According to the GenBank database, the UGE enzyme belongs to a member of the SDR superfamily (Kavanagh et al. 2008). Multiple sequence alignment revealed that the two signature sequences of the SDR superfamily, a GxxGxxG motif (where x is any amino acid), which contains the conserved β-NAD^+ binding domain near the cofactor-binding pocket, and a Ser-Tyr-Lys triad (Ser and YXXXK motif), in which the conserved tyrosine plays a key role in catalysis (Li et al. 2014), were strictly conserved in DoUGE as well as in almost all UGE proteins in monocotyledonous plants such as *O. sativa, Zea mays, Glycine max, Musa acuminata, Elaeis guineensis, Phoenix dactylifera, Sorghum bicolor* and *Brachypodium distachyon* (Fig. 3).

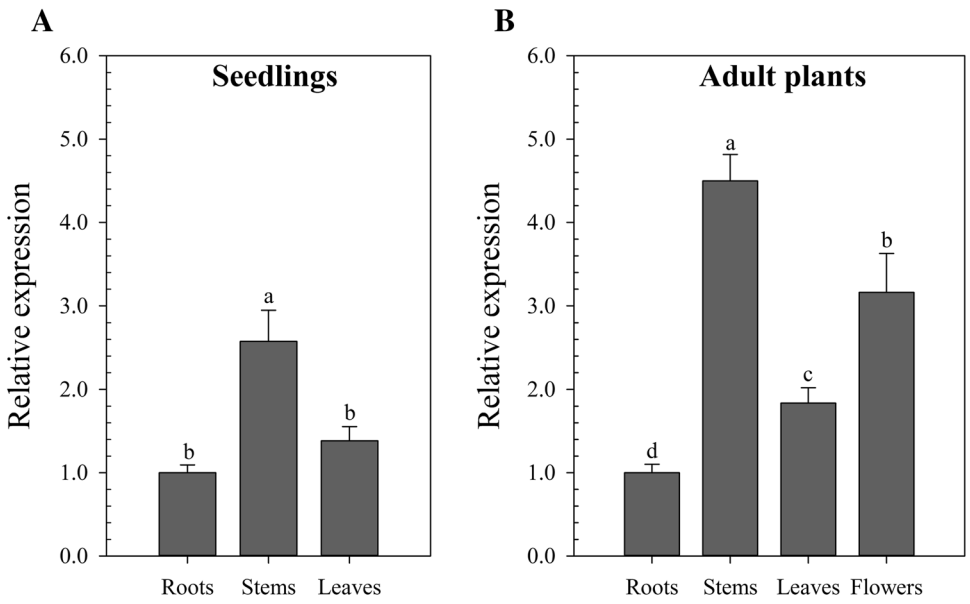

Fig. 6 Tissue-specific expression profiles of *DoUGE* from seedlings and adult plants of *D. officinale*. *D. officinale* seedlings (**a**) were harvested 10 months after germination. Adult *D. officinale* plants (**b**) were collected 14 MAT. Error bars indicate the mean ± standard deviation of three biological replicates. Different letters above bars indicate significant differences by Duncan's multiple range test ($p < 0.05$). *MAT* months after transplantation

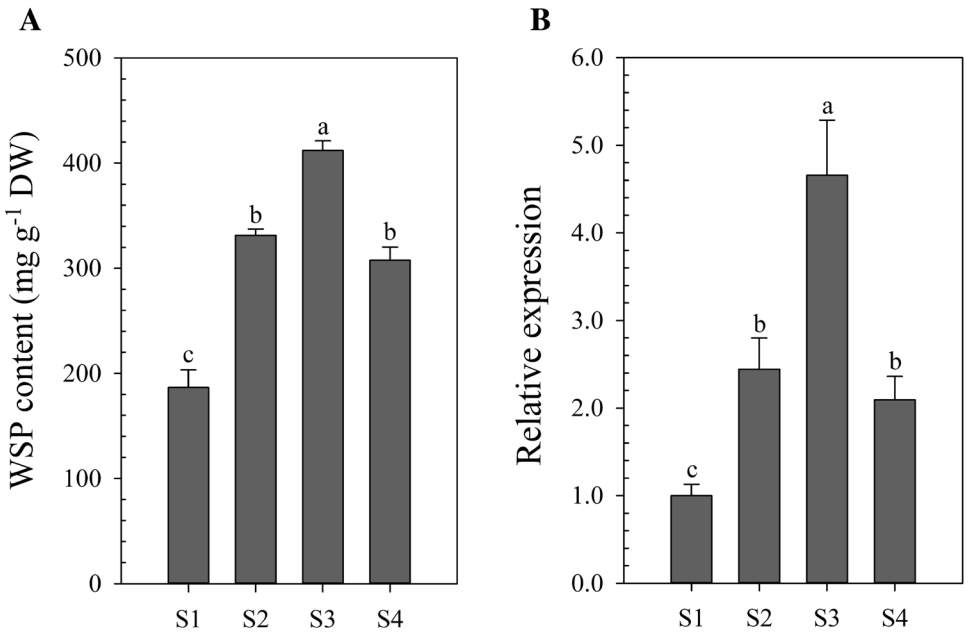

Fig. 7 The content of WSPs (**a**) and expression profiles of *DoUGE* (**b**) from *D. officinale* at four developmental phases: S1 (4 MAT), S2 (8 MAT), S3 (12 MAT), and S4 (16 MAT). Error bars indicate the mean ± standard deviation of three biological replicates. Different letters above bars indicate significant differences by Duncan's multiple range test ($p < 0.05$). *MAT* months after transplantation; *WSPs* water-soluble polysaccharides

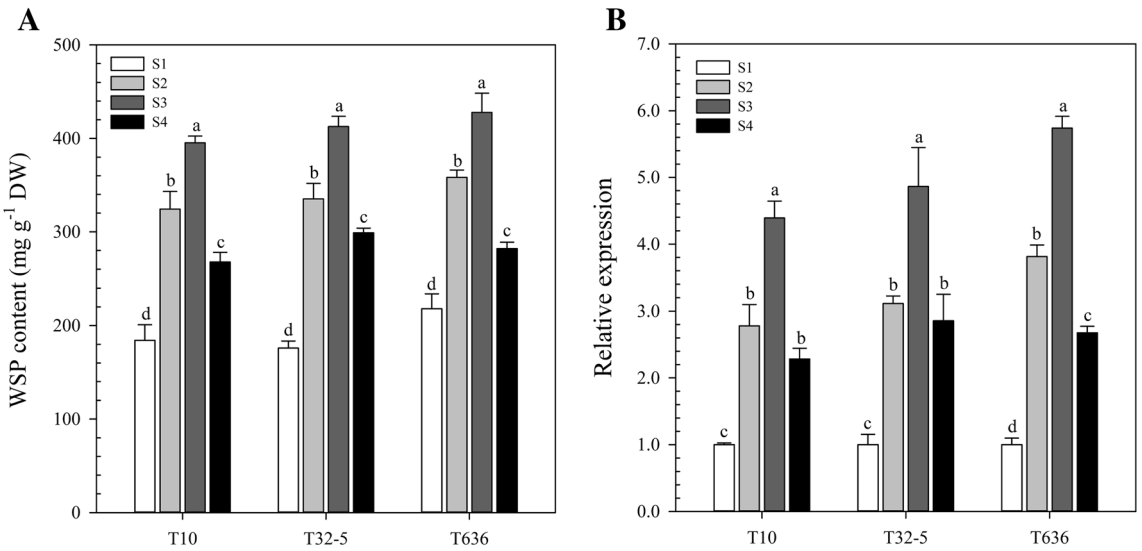

Fig. 8 The content of WSPs (**a**) and expression profiles of *DoUGE* (**b**) in three *D. officinale* genotypes (T10, T32-5 and T6636) at four developmental phases: S1 (4 MAT), S2 (8 MAT), S3 (12 MAT), and S4 (16 MAT). Error bars indicate the mean ± standard deviation of three biological replicates. Different letters above bars indicate significant differences by Duncan's multiple range test ($p < 0.05$). MAT, months after transplantation; WSPs, water-soluble polysaccharides

Accumulation of water-soluble polysaccharides and *DoUGE* expression patterns in *D. officinale*

The key medicinal properties of *D. officinale* have been attributed to the WSPs (Zheng et al. 2012; Teixeira da Silva and Ng 2017), which serve as a promising bioactive material for drugs (Zha et al. 2007; Alonso-Sande et al. 2009). WSPs are considered to be mannan polysaccharides (Xing et al. 2013). *D. officinale* vegetative growth can be completed within a growing season (i.e., one year) (Jiang et al. 2014). Constant plant growth allows WSP content to increase throughout the vegetative growth stage, and thus constant harvesting. However, considerable amounts of WSPs will be consumed during the flowering period, especially hydrolyzed materials from WSPs, including glucose, mannose and galacturonic acid, which become markedly depleted as nutrients (Lin et al. 2009; Jin et al. 2011). To understand the dynamic changes of WSPs in *D. officinale*, WSP content

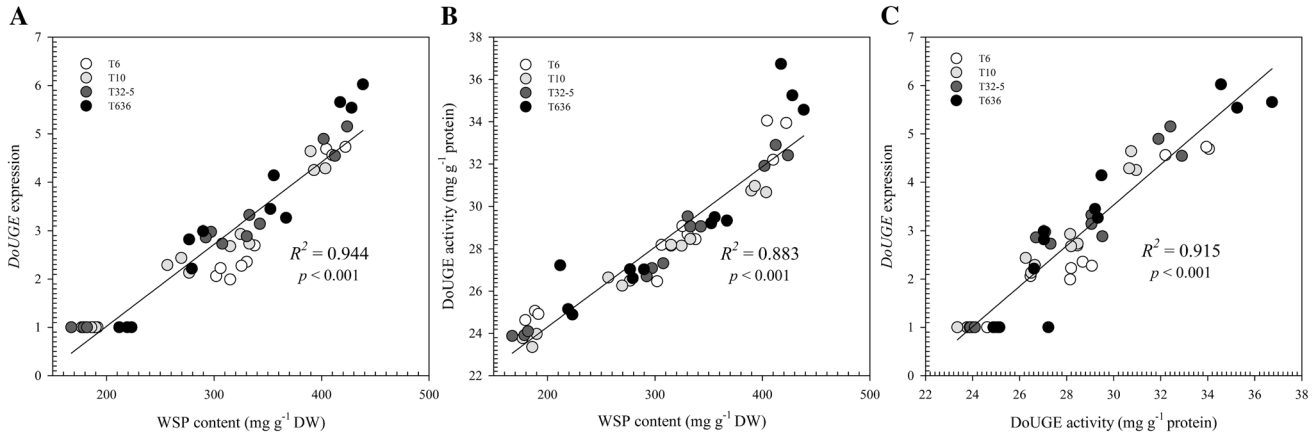

Fig. 9 Pearson's correlations for the accumulation of WSPs, DoUGE activity and *DoUGE* expression in different *D. officinale* genotypes (T6, T10, T32-5 and T636). **a** The relationship between WSP content and *DoUGE* expression. **b** The relationship between WSP content and DoUGE activity. **c** The relationship between WSP content, DoUGE activity and *DoUGE* expression. *WSP* water-soluble polysaccharide

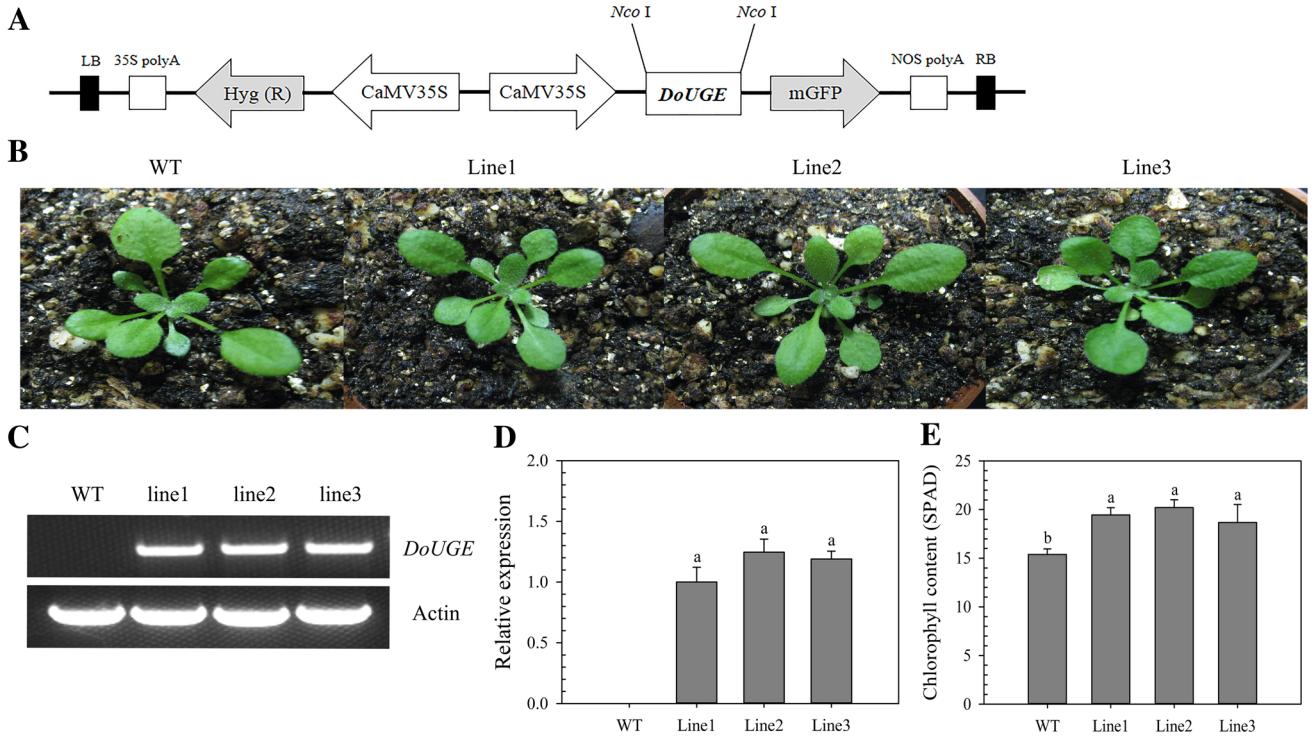

Fig. 10 Overexpression of the *DoUGE* gene in *A. thaliana*. **a** Schematic representation of the *35S::DoUGE* transformation vector under the genetic control of the CaMV-35S promoter. **b** Phenotypic comparison of WT and three transgenic lines 1, 2 and 3 overexpressing *DoUGE* under normal growth conditions. **c** Expression analysis of the *DoUGE* gene in seedlings of WT and three transgenic lines by semi-quantitative RT-PCR. **d** Analysis of the *DoUGE* gene in WT and transgenic lines by qPCR analysis. **e** The chlorophyll content of WT and three transgenic lines. Error bars indicate the mean ± standard deviation of three biological replicates. Different letters above bars indicate significant differences by Duncan's multiple range test ($p < 0.05$). *WT* wild type

was evaluated quarterly for a year (Fig. 7a). There was a significant difference between S1 and S4: lowest in S1, higher in S2, maximum in S3, and rebounding in S4 but less than S2. Furthermore, *D. officinale* WSPs are directly affected by multiple genetic and environmental factors, especially genotype, plant geography, growth duration, harvest period, blossoming, illumination, temperature, and humidity (Xing et al. 2013). Genotype and physiological age affect WSP

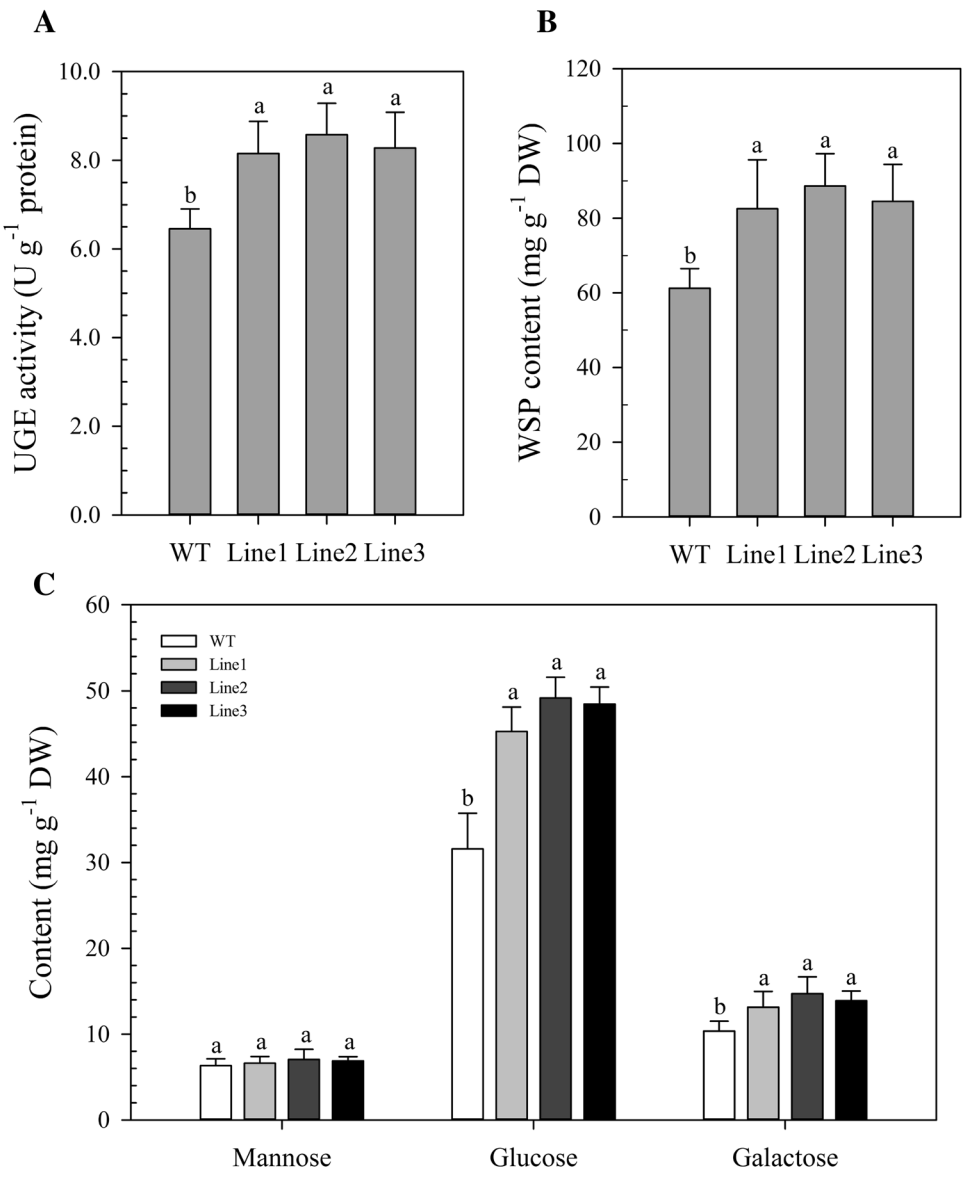

Fig. 11 Quantification of transcription levels and WSP content in one-month old *A. thaliana* seedlings. **a** Analysis of DoUGE activity in WT and transgenic *A. thaliana* plants. **b** Content of WSPs in WT and transgenic lines 1, 2 and 3 overexpressing *DoUGE* under normal growth conditions. **c** Composition of monosaccharides in WSPs of WT and three transgenic lines under normal growth conditions. Error bars indicate the mean ± standard deviation of three biological replicates. Different letters above bars indicate significant differences by Duncan's multiple range test ($p < 0.05$). *WSP* water-soluble polysaccharide, *WT* wild type

content in *D. officinale* (Zhu et al. 2010; Jin et al. 2016). The content of WSPs in three varieties (T10, T32-5 and T636) were different, attributable to different genetic backgrounds, but showed a similar tendency in variation (Fig. 8a). Indeed, the quality of *D. officinale* is primarily determined by the WSP content in the current market (Yan et al. 2015), and the higher the WSP content, the better the quality, indicating that the best harvest period for *D. officinale* is in S3 (Fig. 7a).

Previous studies established that the expression patterns of *DoUGE* in different organs are tightly associated with biological activities and physiological functions (Anderson and Van Itallie 2009). Several homologous genes encoding UGE demonstrate differential gene expression patterns. For instance, *OsUGE*1-4 are expressed in multiple organs of *O. sativa*, with higher expression levels of *OsUGE3* in leaves, seeds and roots than in stems, while highest *OsUGE4* expression is in stems (Kim et al. 2009). *DoUGE* had higher transcript levels in the stems of *D. officinale* seedlings and adult plants, with lower expression in roots, leaves and flowers, which indicated that *DoUGE* might have an essential role to play in plant growth and development (Fig. 6). Given the accumulation of WSPs from S1 to S4, the transcript levels of *DoUGE* first increased then decreased, which corresponded to the content of WSPs at different developmental stages (Fig. 7). qRT-PCR analysis was applied to reveal the dynamic expression profiles of *DoUGE* in three cultivated varieties (Fig. 8b). The transcript levels of *DoUGE* are functionally coherent, so that the up-regulation of *DoUGE* expression is correlated with the increase in WSPs. Furthermore, *UGE* and the gene encoded by

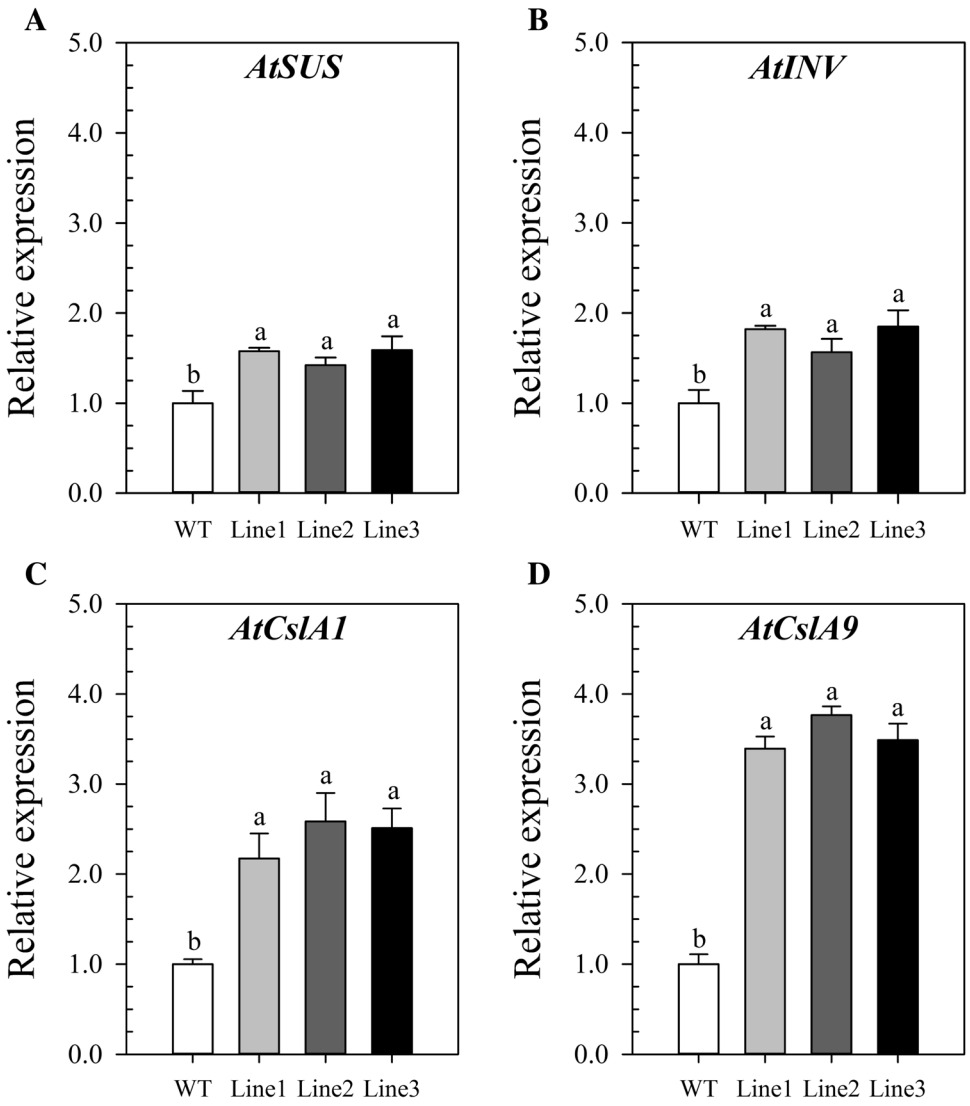

Fig. 12 Expression patterns of four genes (*AtSUS, AtINV, AtCslA1*, and *AtCslA9*) involved in the biosynthesis of WSPs from 1-month-old transgenic lines and WT plants. The expression level of *AtUBQ10* was used as a reference gene to normalize the mRNA levels for each sample. Error bars indicate the mean ± standard deviation of three biological replicates. Different letters above bars indicate significant differences by Duncan's multiple range test ($p < 0.05$). *WSPs* water-soluble polysaccharides, *WT* wild type

mannan synthase are expressed simultaneously, which is consistent with an identical model in *Coffea arabica* (Joet et al. 2014). Eight *DoCslA*s from *D. officinale* displayed the same expression pattern, and accumulated WSPs in the corresponding phase (He et al. 2015), which first increased from S1 to S3 and then decreased in S4, implying that *DoUGE* and *DoCslA* are co-expressed genes involved in the regulation of mannan biosynthesis. A strong correction was observed in different genotypes between WSP content and *DoUGE* expression ($R^2 = 0.94$, $p < 0.001$), WSP content and DoUGE activity ($R^2 = 0.88$, $p < 0.001$), and DoUGE activity and *DoUGE* expression ($R^2 = 0.92$, $p < 0.001$) (Fig. 9). Hence, the expression levels of *DoUGE* appear to be directly associated with the content of WSPs and DoUGE activity in different cultivated varieties during different developmental periods.

Assessment of water-soluble polysaccharides and abiotic stress tolerance in *A. thaliana* transformants

Under normal conditions, the contents of chlorophyll, WSPs, glucose and galactose in transgenic lines were significantly higher than in WT (Figs. 10e, 11b, c). This finding was paralleled with higher expression levels of *DoUGE* (Fig. 9a) and higher UGE activity (Fig. 11a) in transgenic *A. thaliana*. Similarly, *OsUGE1*-overexpressing lines in *O. sativa* contain more soluble sugars, glucose and galactose than WT (Guevara et al. 2014). A strong correlation was found between *DoUGE* transcript levels and WSP content in each transgenic line, corresponding to the results in *D. officinale* (Figs. 6, 7). Thus, the observed increase of WSPs in transgenic plants is closely related to the up-regulated expression of *DoUGE* and the increased UGE activity. Furthermore,

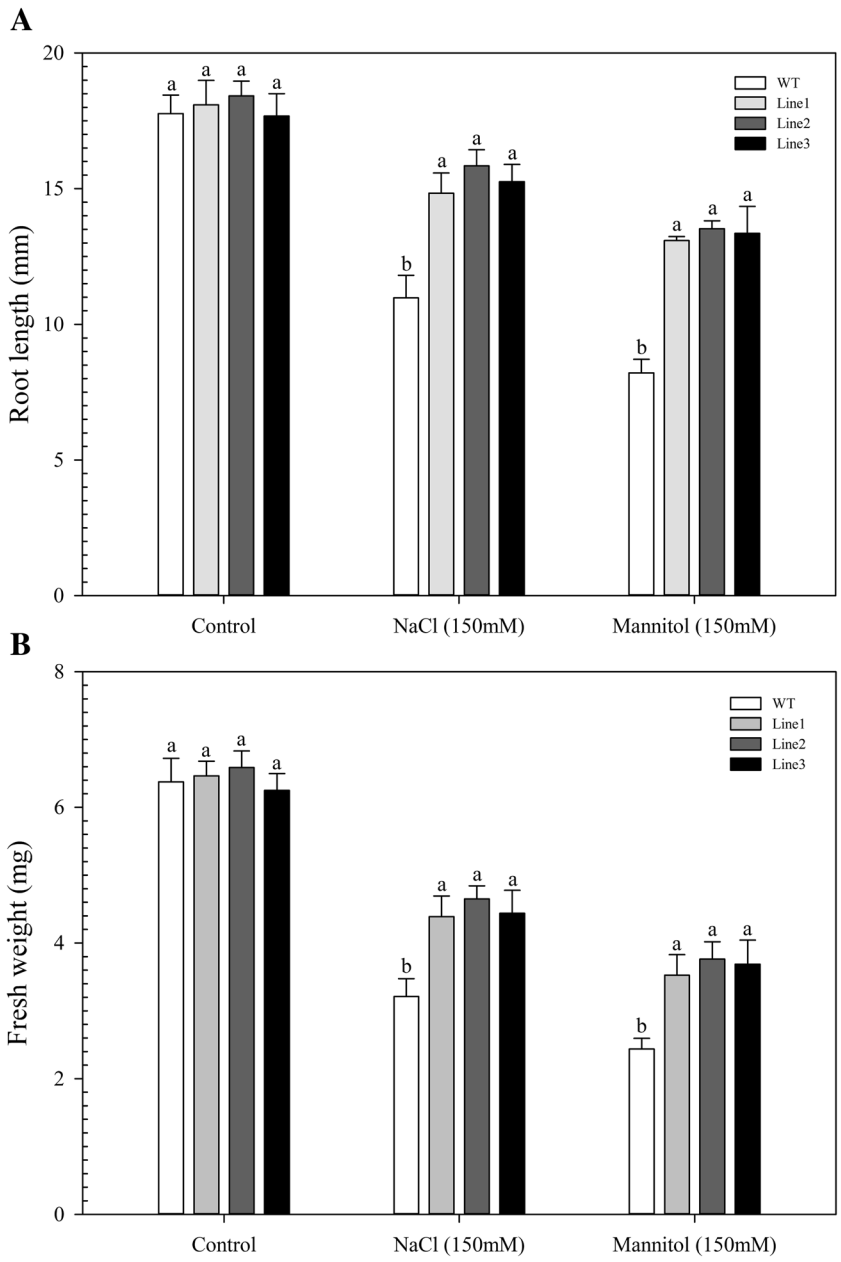

Fig. 13 The role of *DoUGE* in salt and osmotic stresses. **a** Root length of 10-day-old seedlings in transgenic plants (lines 1, 2 and 3) and WT under salt (150 mM NaCl) and osmotic (150 mM mannitol) stress. **b** Fresh weight of 10-day-old seedlings in transgenic plants (three lines) and WT exposed to 150 mM NaCl and 150 mM mannitol. To estimate salt and osmotic stress tolerance, 7-day-old seedlings of WT and *35S::DoUGE* transgenic *A. thaliana* were transferred to fresh half-strength MS medium supplemented with 150 mM NaCl or 200 mM mannitol for an additional 5 days. Error bars indicate the mean ± standard deviation of three biological replicates. Different letters above bars indicate significant differences by Duncan's multiple range test ($p < 0.05$). *WT* wild type

DoUGE exhibited a similar expression profile of multiple genes (including *AtSUS, AtINV, AtCslA1* and *AtCslA9*) associated with WSPs (Fig. 12), suggesting that *DoUGE* was responsible for WSP accumulation during plant growth and development. Agroinfiltration (Ratanasut et al. 2015) could probably be useful for rapid functional analysis of *DoUGE* involved in WSP biosynthesis.

Previously, overexpression of the gene encoding UDP glucose 4-epimerase in transgenic plants such as *A. thaliana* and *Brassica rapa* was shown to be associated with improved tolerance to abiotic stresses (Liu et al. 2007; Jung et al. 2015; Abdula et al. 2016). The *UGE* transcript level is induced by several abiotic stresses, such as high salinity, drought, cold and ABA, which was considered to be involved in expression regulation (Rabbani et al. 2003; Nguyen et al. 2004; Fan et al. 2016). *DoUGE* was found to be up-regulated by salt, drought and SA stresses (Fig. 5), which was supported by the presence of multiple *cis*-regulatory elements conserved in the promoter region (Fig. 4). Moreover, transgenic rice overexpressing *BrUGE* in Yoshida solution supplemented with 250 mM NaCl displayed less growth reduction in roots and shoots compared with WT (Jung et al. 2015). NaCl and mannitol both decrease water potential and induce osmotic stress, which negatively affects plant growth by limiting water uptake, and cell and root growth (Lugan et al. 2010;

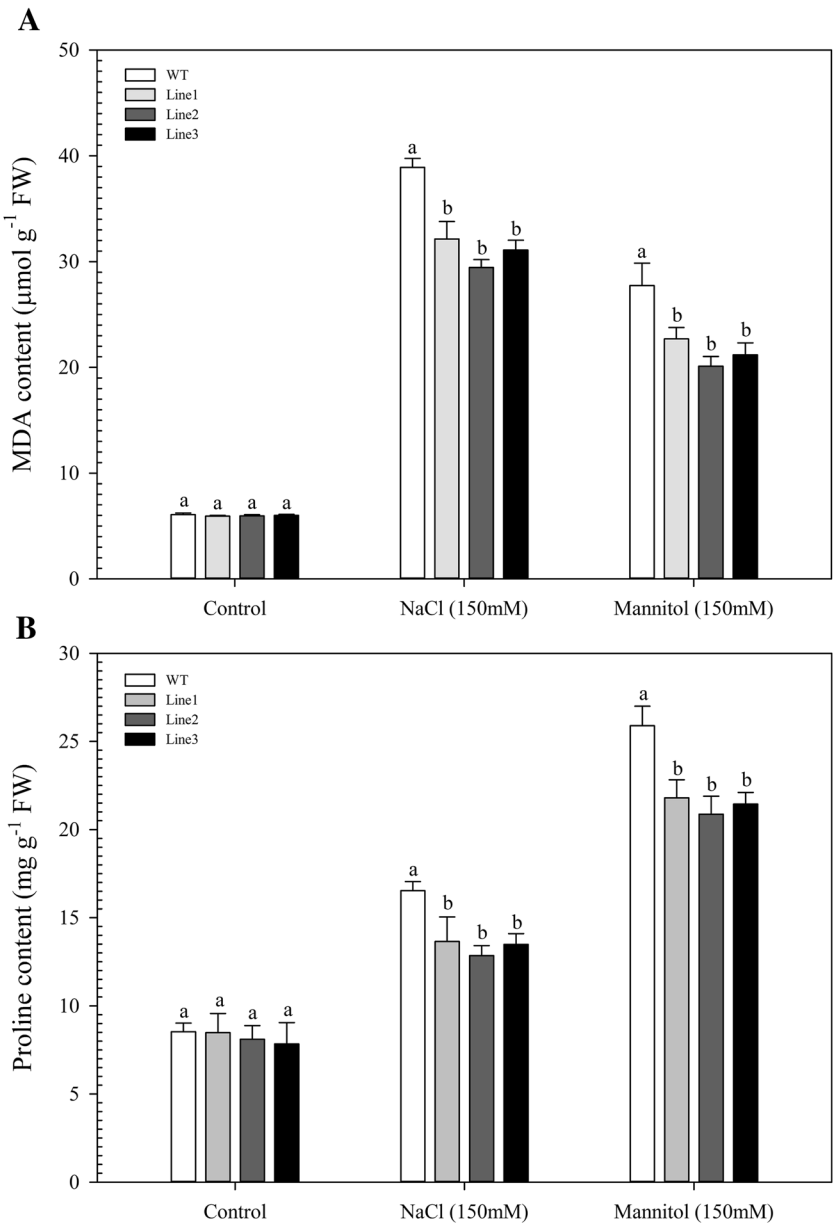

Fig. 14 Measurement of MDA (**a**) and proline contents (**b**) in WT and transgenic *A. thaliana* lines overexpressing *DoUGE* under salt and osmotic stress. To detect MDA and proline contents under salt and osmotic stress, 7-day-old seedlings of WT and *35S::DoUGE* transgenic *A. thaliana* were transferred to fresh half-strength MS medium supplemented with 150 mM NaCl or 200 mM mannitol for an additional 5 days. Error bars indicate the mean ± standard deviation of three biological replicates. Different letters above bars indicate significant differences by Duncan's multiple range test ($p < 0.05$). *MDA* malondialdehyde, *WT* wild type

Zhu et al. 2015). Here, abiotic stress (salinity and osmotic stresses) significantly inhibited the root length and fresh weight of WT and transgenic *A. thaliana* lines, but illustrated an obvious improvement in transgenic lines 1, 2 and 3 compared with WT, indicating that overexpression of *DoUGE* enhanced resistance to salt and osmotic stresses (Fig. 13a, b). Furthermore, the transgenic plants produced more MDA and proline than the WT (Fig. 14), because salt and osmotic stresses result in membrane lipid peroxidation, which causes the accumulation of MDA and proline contents in plants (Levine et al. 1994). DoUGE isoforms affect the production of UDP-glucose and UDP-galactose, the biosynthetic substrates of various carbohydrates, thus improved UGE activity in *A. thaliana* can result in the accumulation of WSPs and subsequently enhanced stress tolerance. Taken together, *DoUGE* induced enhanced tolerance to salt and drought stress, which may result from the bioaccumulation of WSPs.

In conclusion, the *DoUGE* gene and its promoter regions were identified from a precious Chinese herb, *D. officinale*, which is rich in WSPs. Our results provide genetic evidence of the involvement of *DoUGE* in the regulation of WSP content during plant development, as well as in enhanced tolerance to salt and osmotic stresses. Our work highlights a very useful approach to fortify the in planta production of bioactive ingredients and enhanced stress tolerance in crops and medicinal or ornamental plants.

Acknowledgements This work was supported by the Forestry Science and Technology Innovation Fund Project of Guangdong Province (Project Number 2015KJCX040), and the Strategic Priority Research Program of Chinese Academy by the Chinese Academy Sciences (Grant Number KFJ-EW-STS-118).

Author contributions JD and ZY conceived and designed the experiments; ZY performed the experiments with the help of CH, GZ and WD; ZY analyzed the data; JL and JATdS provided important suggestions in data analysis and interpretation; ZY drafted the manuscript; ZY, JATdS and JD revised the manuscript. All authors read and approved this manuscript.

Compliance with ethical standards

Conflict of interest The authors declare no conflicts of interest.

References

Abdula SE, Lee HJ, Kim J, Nino MC, Jung YJ, Cho YC, Nou I, Kang KK, Cho YG (2016) *BrUGE1* transgenic rice showed improved growth performance with enhanced drought tolerance. Breed Sci 66(2):226–233

Alonso-Sande M, Teijeiro-Osorio D, Remunan-Lopez C, Alonso MJ (2009) Glucomannan, a promising polysaccharide for biopharmaceutical purposes. Eur J Pharm Biopharm 72(2):453–462

Anderson JM, Van Itallie CM (2009) Physiology and function of the tight junction. Cold Spring Harbor Perspect Biol 1(2):a002584

Barber C, Rosti J, Rawat A, Findlay K, Roberts K, Seifert GJ (2006) Distinct properties of the five UDP-D-glucose/UDP-D-galactose 4-epimerase isoforms of *Arabidopsis thaliana*. J Biol Chem 281(25):17276–17285

Bari R, Jones JDG (2009) Role of plant hormones in plant defence responses. Plant Mol Biol 69(4):473–488

Beerens K, Soetaert W, Desmet T (2015) UDP-hexose 4-epimerases: a view on structure, mechanism and substrate specificity. Carbohydr Res 414:8–14

Citovsky V, Lee LY, Vyas S, Glick E, Chen MH, Vainstein A, Gafni Y, Gelvin SB, Tzfira T (2006) Subcellular localization of interacting proteins by bimolecular fluorescence complementation *in planta*. J Mol Biol 362(5):1120–1131

Clough SJ, Bent AF (1998) Floral dip: a simplified method for *Agrobacterium*-mediated transformation of *Arabidopsis thaliana*. Plant J 16(6):735–743

Diaz de Leon F, Klotz KL, Lagrimini LM (1993) Nucleotide sequence of the tobacco (*Nicotiana tabacum*) anionic peroxidase gene. Plant Physiol 101(3):1117–1118

Dormann P, Benning C (1998) The role of UDP-glucose epimerase in carbohydrate metabolism of *Arabidopsis*. Plant J 13(5):641–652

Dubois M, Gilles KA, Hamilton JK, Rebers PA, Smith F (1956) Colorimetric method for determination of sugars and related substances. Anal Chem 28(3):350–356

Dubos C, Stracke R, Grotewold E, Weisshaar B, Martin C, Lepiniec L (2010) MYB transcription factors in *Arabidopsis*. Trends Plant Sci 15(10):573–581

El-Ganiny AM, Sheoran I, Sanders DA, Kaminskyj SG (2010) *Aspergillus nidulans* UDP-glucose-4-epimerase UgeA has multiple roles in wall architecture, hyphal morphogenesis, and asexual development. Fungal Genet Biol 47(7):629–635

Fan H, Wu Q, Wang X, Wu L, Cai Y, Lin Y (2016) Molecular cloning and expression of 1-deoxy-D-xylulose-5-phosphate synthase and 1-deoxy-D-xylulose-5-phosphate reductoisomerase in *Dendrobium officinale*. Plant Cell Tiss Org Cult 125(2):381–385

Gao F, Cao XF, Si JP, Chen ZY, Duan CL (2016) Characterization of the alkaline/neutral invertase gene in *Dendrobium officinale* and its relationship with polysaccharide accumulation. Genet Mol Res 15(2):1–8

Gondolf VM, Stoppel R, Ebert B, Rautengarten C, Liwanag AJ, Loque D, Scheller HV (2014) A gene stacking approach leads to engineered plants with highly increased galactan levels in *Arabidopsis*. BMC Plant Biol 14:344

Guevara DR, El-Kereamy A, Yaish MW, Mei-Bi Y, Rothstein SJ (2014) Functional characterization of the rice UDP-glucose 4-epimerase 1, *OsUGE1*: a potential role in cell wall carbohydrate partitioning during limiting nitrogen conditions. PLoS ONE 9(5):e96158

Harrison SJ, Mott EK, Parsley K, Aspinall S, Gray JC, Cottage A (2006) A rapid and robust method of identifying transformed *Arabidopsis thaliana* seedlings following floral dip transformation. Plant Methods 2:19

He C, Zhang J, Liu X, Zeng S, Wu K, Yu Z, Wang X, Teixeira da Silva JA, Lin Z, Duan J (2015) Identification of genes involved in biosynthesis of mannan polysaccharides in *Dendrobium officinale* by RNA-seq analysis. Plant Mol Biol 88(3):219–231

He C, Wu K, Zhang J, Liu X, Zeng S, Yu Z, Zhang X, Teixeira da Silva JA, Deng R, Tan J, Luo J, Duan J (2017a) Cytochemical localization of polysaccharides in *Dendrobium officinale* and the involvement of *DoCSLA6* in the synthesis of mannan polysaccharides. Front Plant Sci 8:173

He C, Zeng S, Teixeira da Silva JA, Yu Z, Tan J, Duan J (2017b) Molecular cloning and functional analysis of the *phosphomannomutase* (*PMM*) gene from *Dendrobium officinale* and evidence for the involvement of an abiotic stress response during germination. Protoplasma 254(4):1693–1704

Holden HM, Rayment I, Thoden JB (2003) Structure and function of enzymes of the Leloir pathway for galactose metabolism. J Biol Chem 278(45):43885–43888

Jiang W, Jiang B, Mantri N, Wu ZG, Mao LZ, Lu HF, Tao ZM (2014) Comparative ecophysiological analysis of photosynthesis, biomass allocation, polysaccharide and alkaloid content in three *Dendrobium candidum* cultivars. Plant Omics 7(2):117–122

Jin X, Yuan H, Si J, Zhang Z, Yu Q, Wang L (2011) Effect of blossom on the content of polysaccharide and monosaccharide components in *Dendrobium officinale*. China. J Chinese Materia Med 36(16):2176–2178

Jin Q, Jiao C, Sun S, Song C, Cai Y, Lin Y, Fan H, Zhu Y (2016) Metabolic analysis of medicinal *Dendrobium officinale* and *Dendrobium huoshanense* during different growth years. PloS ONE 11(1):e0146607

Joet T, Laffargue A, Salmona J, Doulbeau S, Descroix F, Bertrand B, Lashermes P, Dussert S (2014) Regulation of galactomannan biosynthesis in coffee seeds. J Exp Bot 65(1):323–337

Jung YJ, Kyoung JH, Nou IS, Cho YG, Kang KK (2015) Molecular characterization of the UDP-glucose 4-epimerase (*BrUGE*) gene family in response to biotic and abiotic stress in Chinese cabbage (*Brassica rapa*). Plant Biotechnol Rep 9(6):339–350

Jyothishwaran G, Kotresha D, Selvaraj T, Srideshikan SM, Rajvanshi PK, Jayabaskaran C (2007) A modified freeze-thaw method for efficient transformation of *Agrobacterium tumefaciens*. Curr Sci 93(6):770–772

Kavanagh KL, Jornvall H, Persson B, Oppermann U (2008) Medium- and short-chain dehydrogenase /reductase gene and protein families: the SDR superfamily: functional and structural diversity within a family of metabolic and regulatory enzymes. Cell Mol Life Sci 65(24):3895–3906

Kim SK, Kim DH, Kim BG, Jeon YM, Hong BS, Ahn JH (2009) Cloning and characterization of the UDP glucose/galactose epimerases of *Oryza sativa*. J Korean Soc Appl Biol Chem 52(4):315–320

Levine A, Tenhaken R, Dixon R, Lamb C (1994) H_2O_2 from the oxidative burst orchestrates the plant hypersensitive disease resistance response. Cell 79(4):583–593

Li C, Wang Y, Liu L, Hu Y, Zhang F, Mergen S, Wang G, Schlappi MR, Chu C (2011) A rice plastidial nucleotide sugar epimerase is involved in galactolipid biosynthesis and improves photosynthetic efficiency. PLoS Genet 7(7):e1002196

Li CT, Liao CT, Du SC, Hsiao YP, Lo HH, Hsiao YM (2014) Functional characterization and transcriptional analysis of *galE* gene encoding a UDP-galactose 4-epimerase in *Xanthomonas campestris* pv. *campestris*. Microbiol Res 169(5–6):441–452

Lin Y, Zeng S, Han D, Sun J (2009) Study on the variation of water-soluble polysaccharides content of *Dendrobium candidum* Wall. Ex Lindl Res Pract Chin Med 23(2):19–21

Ling Q, Huang W, Jarvis P (2011) Use of a SPAD-502 m to measure leaf chlorophyll concentration in *Arabidopsis thaliana*. Photosynth Res 107(2):209–214

Liu HL, Dai XY, Xu YY, Chong K (2007) Over-expression of *OsUGE-1* altered raffinose level and tolerance to abiotic stress but not morphology in *Arabidopsis*. J Plant Physiol 164(10):1384–1390

Lu YQ, Jia Q, Tong ZK (2014) Cloning and sequence analysis of nine novel *MYB* genes in Taxodiaceae plants. J Forest Res 25(4):795–804

Lugan R, Niogret MF, Leport L, Guegan JP, Larher FR, Savoure A, Kopka J, Bouchereau A (2010) Metabolome and water homeostasis analysis of *Thellungiella salsuginea* suggests that dehydration tolerance is a key response to osmotic stress in this halophyte. Plant J 64(2):215–229

Maitra US, Ankel H (1971) Uridine diphosphate-4-keto-glucose, an intermediate in the uridine diphosphate-galactose-4-epimerase reaction. Proc Natl Acad Sci USA 68(11):2660–2663

Majumdar S, Ghatak J, Mukherji S, Bhattacharjee H, Bhaduri A (2004) UDP-galactose 4-epimerase from *Saccharomyces cerevisiae*. A bifunctional enzyme with aldose 1-epimerase activity. Eur J Biochem 271(4):753–759

Michiels A, Tucker M, Van den Ende W, Van Laere A (2003) Chromosomal walking of flanking regions from short known sequences in GC-rich plant genomic DNA. Plant Mol Biol Rep 21(3):295–302

Miyawaki A, Llopis J, Heim R, McCaffery JM, Adams JA, Ikura M, Tsien RY (1997) Fluorescent indicators for Ca^{2+} based on green fluorescent proteins and calmodulin. Nature 388(6645):882–887

Murashige T, Skoog F (1962) A revised medium for rapid growth and bio assays with tobacco tissue cultures. Physiol Plantarum 15(3):473–497

Ng TB, Liu J, Wong JH, Ye X, Wing Sze SC, Tong Y, Zhang KY (2012) Review of research on *Dendrobium*, a prized folk medicine. Appl Microbiol Biot 93(5):1795–1803

Nguyen TT, Klueva N, Chamareck V, Aarti A, Magpantay G, Millena AC, Pathan MS, Nguyen HT (2004) Saturation mapping of QTL regions and identification of putative candidate genes for drought tolerance in rice. Mol Genet Genomics 272(1):35–46

Niou YK, Wu WL, Lin LC, Yu MS, Shu HY, Yang HH, Lin GH (2009) Role of *galE* on biofilm formation by *Thermus* spp. Biochem Biophys Res Commun 390(2):313–318

Rabbani MA, Maruyama K, Abe H, Khan MA, Katsura K, Ito Y, Yoshiwara K, Seki M, Shinozaki K, Yamaguchi-Shinozaki K (2003) Monitoring expression profiles of rice genes under cold, drought, and high-salinity stresses and abscisic acid application using cDNA microarray and RNA get-blot analyses. Plant Physiol 133(4):1755–1767

Ratanasut K, Monmai C, Piluk P (2015) Transient hairpin RNAi-induced silencing in floral tissues of *Dendrobium* Sonia 'Earsakul' by agroinfiltration for rapid assay of flower colour modification. Plant Cell Tiss Org Cult 120(2):643–654

Reiter WD, Vanzin GF (2001) Molecular genetics of nucleotide sugar interconversion pathways in plants. Plant Mol Biol 47(1–2):95–113

Rosti J, Barton CJ, Albrecht S, Dupree P, Pauly M, Findlay K, Roberts K, Seifert GJ (2007) UDP-glucose 4-epimerase isoforms UGE2 and UGE4 cooperate in providing UDP-galactose for cell wall biosynthesis and growth of *Arabidopsis thaliana*. Plant Cell 19(5):1565–1579

Saitou N, Nei M (1987) The neighbor-joining method: a new method for reconstructing phylogenetic trees. Mol Biol Evol 4(4):406–425

Schmittgen TD, Livak KJ (2008) Analyzing real-time PCR data by the comparative C_T method. Nat Protoc 3(6):1101–1108

Seifert GJ, Barber C, Wells B, Dolan L, Roberts K (2002) Galactose biosynthesis in *Arabidopsis*: Genetic evidence for substrate channeling from UDP-D-galactose into cell wall polymers. Curr Biol 12(21):1840–1845

Tamirisa S, Vudem DR, Khareedu VR (2014) Overexpression of pigeonpea stress-induced cold and drought regulatory gene (*CcCDR*) confers drought, salt, and cold tolerance in *Arabidopsis*. J Exp Bot 65(17):4769–4781

Tamura K, Stecher G, Peterson D, Filipski A, Kumar S (2013) MEGA6: molecular evolutionary genetics analysis version 6.0. Mol Biol Evol 30(12):2725–2729

Teixeira da Silva JA, Ng TB (2017) The medicinal and pharmaceutical importance of *Dendrobium* species. Appl Microbiol Biotechnol 101(6):2227–2239

Thompson JD, Gibson TJ, Plewniak F, Jeanmougin F, Higgins DG (1997) The CLUSTAL_X windows interface: flexible strategies for multiple sequence alignment aided by quality analysis tools. Nucleic Acids Res 25(24):4876–4882

Walther D, Brunnemann R, Selbig J (2007) The regulatory code for transcriptional response diversity and its relation to genome structural properties in *A. thaliana*. PLoS Genet 3(2):e11

Wan RL, Sun J, He T, Hu YD, Zhao Y, Wu Y, Chun Z (2016) Cloning cDNA and functional characterization of UDP-glucose pyrophosphorylase in *Dendrobium officinale*. Biol Plantarum 61(1):147–154

Wang Y, Alonso AP, Wilkerson CG, Keegstra K (2012) Deep EST profiling of developing fenugreek endosperm to investigate galactomannan biosynthesis and its regulation. Plant Mol Biol 79(3):243–258

Wu FH, Shen SC, Lee LY, Lee SH, Chan MT, Lin CS (2009) Tape-*Arabidopsis* Sandwich - a simpler *Arabidopsis* protoplast isolation method. Plant Methods 5:16

Xing X, Cui SW, Nie S, Phillips GO, Goff HD, Wang Q (2013) A review of isolation process, structural characteristics, and bioactivities of water-soluble polysaccharides from *Dendrobium* plants. Bioact Carbohydrates Diet Fiber 1(2):131–147

Yan L, Wang X, Liu H, Tian Y, Lian J, Yang R, Hao S, Wang X, Yang S, Li Q, Qi S, Kui L, Okpekum M, Ma X, Zhang J, Ding Z, Zhang G, Wang W, Dong Y, Sheng J (2015) The genome of *Dendrobium officinale* illuminates the biology of the important traditional Chinese orchid herb. Mol Plant 8(6):922–934

Yin Y, Huang J, Gu X, Bar-Peled M, Xu Y (2011) Evolution of plant nucleotide-sugar interconversion enzymes. PLoS ONE 6(11):e27995

Yoo SD, Cho YH, Sheen J (2007) *Arabidopsis* mesophyll protoplasts: a versatile cell system for transient gene expression analysis. Nat Protoc 2(7):1565–1572

Yun YH, Wei YC, Zhao XB, Wu WJ, Liang YZ, Lu HM (2015) A green method for the quantification of polysaccharides in *Dendrobium officinale*. RSC Adv 5(127):105057–105065

Zha XQ, Luo JP, Luo SZ, Jiang ST (2007) Structure identification of a new immunostimulating polysaccharide from the stems of *Dendrobium huoshanense*. Carbohyd Polym 69(1):86–93

Zhang X, Henriques R, Lin SS, Niu QW, Chua NH (2006) *Agrobacterium*-mediated transformation of *Arabidopsis thaliana* using the floral dip method. Nat Protoc 1(2):641–646

Zhang ZJ, Wang J, Zhang RX, Huang RF (2012) The ethylene response factor *AtERF98* enhances tolerance to salt through the transcriptional activation of ascorbic acid synthesis in *Arabidopsis*. Plant J 71(2):273–287

Zhang GQ, Xu Q, Bian C, Tsai WC, Yeh CM, Liu KW, Yoshida K, Zhang LS, Chang SB, Chen F, Shi Y, Su YY, Zhang YQ, Chen LJ, Yin Y, Lin M, Huang H, Deng H, Wang ZW, Zhu SL, Zhao X, Deng C, Niu SC, Huang J, Wang M, Liu GH, Yang HJ, Xiao XJ, Hsiao YY, Wu WL, Chen YY, Mitsuda N, Ohme-Takagi M, Luo YB, Van de Peer Y, Liu ZJ (2016a) The *Dendrobium catenatum* Lindl. genome sequence provides insights into polysaccharide synthase, floral development and adaptive evolution. Sci Rep 6:19029

Zhang J, He C, Wu K, Teixeira da Silva JA, Zeng S, Zhang X, Yu Z, Xia H, Duan J (2016b) Transcriptome analysis of *Dendrobium officinale* and its application to the identification of genes associated with polysaccharide synthesis. Front Plant Sci 7:5

Zheng YP, Jiang W, Silva EN, Mao LZ, Hannaway DB, Lu HF (2012) Optimization of shade condition and harvest time for *Dendrobium candidum* plants based on leaf gas exchange, alkaloids and polysaccharides contents. Plant Omics 5(3):253–260

Zhu Y, Si J, Guo B, He B, Zhang A (2010) Quantitive variation of polysaccharides content in cultivated *Dendrobium candidum*. China J Chin Materia Med 35(4):427–430

Zhu YX, Xu XB, Hu YH, Han WH, Yin JL, Li HL, Gong HJ (2015) Silicon improves salt tolerance by increasing root water uptake in *Cucumis sativus* L. Plant Cell Rep 34(9):1629–1646